Fragmentation mechanisms of α-amino acids protonated under electrospray ionization: a collisional activation and ab initio theoretical study

Françoise Rogalewicz, Yannik Hoppilliard*, Gilles Ohanessian

DCMR, UMR CNRS 7651, Ecole Polytechnique, 91128 Palaiseau Cedex, France

Abstract

The ionic complexes formed by electrospray of methanol/water solutions of all the α amino acids (AA) were studied by collisional activation in a triple quadrupole mass spectrometer. The fragmentation common to all protonated AA, except tryptophan, lysine, and arginine, is the well known sequential loss of H_2O and CO yielding an immonium ion. For $GlyH^+$ it is argued that formation of $CH_2NH_2^+$ involves the most stable N-protonated form from which a proton is transferred to the hydroxy group. For the amino acids bearing a functional group on their side chain, formation of the immonium ion is in competition either with the loss of ammonia from the amino terminus or with the loss of a small molecule from the side chain. Extensive ab initio calculations at the MP2/6-31G* level have been carried out to determine the various fragmentation pathways of $SerH^+$ and $CysH^+$. These calculations are further used to validate an empirical determination of thermochemical data based on experimental heats of formation and Benson increments. Such approximate data are used to interpret the fragmentations of protonated Met, Thr, Asn, Asp, Gln, and Glu. They are in agreement with an initial protonation at the N terminus of these amino acids. On the other hand, side chain protonation is expected to occur for His, Trp, Lys, and Arg. With increasing collision energy, proton transfer to less basic sites X (X = SH, SCH_3, OH, NH_2 . . .) can occur. All primary fragmentations start with an elongation of the $C-^+XH$ bond. This elongation may be assisted by a cyclisation stabilizing the incoming carbocation. The competitive fragmentations of each protonated amino acid are governed by a combination of enthalpic factors [bond dissociation energies (BDE) of the various $C-^+XH$ bonds and the energy of the final states associated with each HX loss] and activation barriers associated with rearrangements. (Int J Mass Spectrom 195/196 (2000) 565–590) © 2000 Elsevier Science B.V.

Keywords: Fragmentation mechanisms; Amino acids; Electrospray; Ab initio calculations

1. Introduction

The electrospray of methanol-water solutions of all 20 α-amino acids (AA) constitutive of the proteins of living systems leads to the formation of protonated species. For about 30 years, the gas phase chemistry of protonated AA (AAH$^+$) has received great interest. Most of the ionization techniques available on commercial mass spectrometers have been used to generate these protonated species: chemical ionization (CI) [1–6 and references cited therein], secondary ion mass spectrometry (SIMS) [7–9], fast atom bombard-

---

*Corresponding author.

Dedicated to Bob Squires for his many seminal contributions to mass spectrometry and ion chemistry.

ment (FAB) [6,10–12], laser desorption (LD) [13,14], and plasma desorption (PD) [5,15]. However, to the best of our knowledge, the mass spectra of AA ionized under electrospray conditions have not been described, except for glycine (Gly) [16].

We present herein a study of the decomposition processes of AAH^+ by MS/MS in a triple quadrupole instrument. A common assumption in the literature is that the protonated species obtained by various desorption-ionization or desolvation-ionization techniques are in their most stable form. However, many of the commonly observed fragmentations require protonation of less basic sites. This has led to the mobile proton model [17], in which the protonating hydrogen is able to sample all positions bearing labile hydrogens before fragmentation. However, protonation of each of the various basis sites available in each AA could lead to many decomposition products, not all of which are observed. The purpose of this study is the determination of the factors governing the competition between fragmentations of AAH^+ induced by low energy collisions.

2. Experimental and computational

2.1. Materials

The twenty α-amino acids were purchased from Aldrich Chemical (St Quentin Fallavier, France) and used as received without further purification. Sample solutions were prepared in a 50/50 v/v aqueous methanol solvent by dissolving the amino acid to achieve a 500 μM concentration. All solvents used were high-performance liquid chromatography (HPLC) grade. In these conditions the pH of the electrosprayed solutions is close to neutrality (pH = 6–6.5). H/D exchange was carried out by using a 50/50 v/v D_2O and MeOD mixture as solvent. All solutions were infused at a flow rate of 10 μl/mm by a Harvard Apparatus (South Natick, MA, USA) syringe pump.

2.2. Mass spectrometry

All mass spectra were acquired on a Quattro II (Micromass, Manchester, UK) triple quadrupole elec-

trospray mass spectrometer. Typical optimized values for source parameters were: capillary 2.5–3.5 kV, counter electrode 0.1–0.3 kV, temperature 80 °C, RF lens 0.7 V, skimmer 1.5 V, skimmer lens offset 5 V. Resolution was adjusted to optimize the intensity of the precursor ion signal. For the same purpose, the cone voltage was set to 35 V. Collision induced dissociation (CID) was achieved with argon as the target gas. The collision energy in the laboratory frame, E_{lab}, was fixed at $\sim$12 eV and the gas pressure adjusted to achieve a 30–50% transmittance of the precursor ion. The resulting CID spectra are gathered in Table 1.

Typical CID spectra of the type described above are useful to establish the main fragmentation trends. However, many AAH^+ display fairly complex dissociation patterns, which strongly depend upon their internal energies. Therefore, it was deemed important to follow the energy dependence of the CID spectra by varying the kinetic energy in the collision cell. Although the internal energy content of the parent ions are somewhat ill-defined in these experiments, the resulting breakdown graphs (see Figs. 1, 2, and 10 for $SerH^+$, $CysH^+$, and $TrpH^+$, respectively) provide much more detailed information on AAH^+ fragmentations. Such experiments were carried out for most AAH^+. Because analogous graphs have already been published for several other AAH^+ by Harrison and co-workers [12], the information was not duplicated.

2.3. Ab initio calculations and empirical thermochemical estimates

All calculations were carried out at the MP2(FC)/6-31G* level, for both geometry optimizations and vibrational frequency calculations, using the Gaussian94 package [18]. Core orbitals frozen in the MP2 calculations were the 1s of C, N, O, and S. For many of the minima investigated, several conformations were computed. Results will only be described for the most stable conformer of each species. Transition states were identified as stationary points with one imaginary frequency. The appropriate nature of the transition vector was identified by graphical animation using either the Molden [19] or Xmol [20]

programs. For larger AAs, ab initio calculations are excessively CPU time consuming. Therefore, reaction enthalpies and approximate activation energies were obtained from experimental formation enthalpies [21] whenever available, or combined with approximate values obtained using Benson increments [22]. The details of such evaluations is given in the corresponding table captions.

3. Results and discussion

At low cone voltages, the electrospray of methanol-water solutions of each amino acid leads to the formation of protonated complexes of the form $[(AA)_nH]^+$ ($n = 1–3$), and of solvated molecular ions. At higher cone voltages, dissociation of these ions leads to formation of AAH^+. In order to optimize the intensity of the AAH^+ ion signal, the cone voltage was set to 35 V. Table 1 gives the low energy CID ($E_{lab} = 12$ eV in the collision cell) of AAH^+. The shifts of parent and fragment ions masses after total H/D exchange of the labile hydrogens in the molecular ions are also given in this table.

Loss of (C, H_2, O_2)

Table 1 shows the $[AAH-46]^+$ ion as an abundant fragment ion in the spectra of all AAH^+ except for Trp, Lys, and Arg. This is consistent with previous observations for Trp [7,11–13,15], Lys [11–12,15], and Arg [7–8,10–12,15]. Whatever the ionization technique [1–16], this fragmentation was observed earlier in the mass spectra of AAH^+ having enough internal energy to fragment; it is the main or one of the main decomposition processes of these species. This has been confirmed quantitatively for $GlyH^+$ by Klassen and Kebarle [16]. These authors have determined the formation threshold for each of the fragment ions of energized $GlyH^+$, showing $NH_2CH_2^+$ to be the fragment of smallest critical energy: 186 kJ/mol. The mechanism currently admitted is the consecutive loss of water and carbon monoxide. Arguments in favor of this pathway come from either

thermochemical data or mass spectrometric results [4–6].

3.1. Glycine

In this section, arguments are given to show that the consecutive losses of H_2O and CO, the major fragmentation observed in the CID of $GlyH^+$ at $E_{lab} = 12$ eV (Table 1), proceeds from its most stable structure, which is the N-protonated form.

Several ab initio calculations [23–26] were performed to determine the proton affinity (PA) of Gly and the relative energies of the various isomers of $GlyH^+$. They all give the N-protonated form as the most stable one in agreement with the well known basicity of primary amines versus carboxylic acids. However, few of these studies considered the PA differences between the three sites of protonation available in Gly, which are: (1) the amino nitrogen (N); (2) the carbonyl oxygen (CO); and (3) the hydroxyl oxygen (OH). Literature values are gathered in Table 2.

The best precursor for an initial loss of water is the glycine protonated on the hydroxyl oxygen. For such a structure, ab initio calculations [23,26] reveal the formation of an ion–dipole complex $[NH_2CH_2C(O)–OH_2]^+$ prefiguring an impending loss of water, which can then be followed by CO elimination. However, if protonated glycine is initially formed in its most stable structure, consecutive losses of H_2O and CO require three steps: (1) proton transfer from N to OH; (2) simple cleavage of the $C(O)–^+OH_2$ bond; and (3) simple cleavage of the $NH_2CH_2^+–C=O$ bond. The transition state associated with the first step has been calculated to lie only 6 kJ/mol higher in energy than the OH-protonated form [26]. Consequently, the activation energy associated with the N to OH proton transfer is close to the PA difference between these two protonation sites. This result will be used later in the interpretation of the fragmentations of other amino acids.

In the ion–dipole complex $[NH_2CH_2C(O)–OH_2]^+$ depicting the OH protonated form, the $C(O)–^+OH_2$ bond is much longer than the C(O)–OH bond in neutral glycine (2.1 versus 1.36 Å [23], and 2.35

Table 1
Low energy CID (E_{lab}=12 eV) mass spectra of protonated amino acids: m/z ratios, H/D exchange shifts (in italics), and relative ion intensities (in parentheses). Only ion intensities exceeding 10% of the base peak are listed

Amino acid	Precursor ion AAH$^+$	Fragments			Other fragments			
		−NH$_3$	−H$_2$O	−H$_2$O, CO				
Gly	76 + *4* (100%)			30 + *2* (70%)	48 + *4* (10%)			
Ala	90 + *4* (100%)			44 + *2* (90%)				
Val	118 + *4* (100%)			72 + *2* (80%)				
Leu	132 + *4* (100%)			86 + *2* (75%)				
Ile	132 + *4* (100%)			86 + *2* (80%)				
Pro	116 + *3* (100%)			70 + *1* (80%)				
Ser	106 + *5* (100%)		88 + *3* (18%)	60 + *3* (80%)	70 + *1* (10%)			
Thr	120 + *5* (100%)		102 + *3* (35%)	74 + *3* (60%)	84 + *1* (10%)	56 + *1* (10%)		
Asp	134 + *5* (100%)		116 + *3* (45%)	88 + *3* (90%)	74 + *3* (50%)			
Glu	148 + *5* (100%)		130 + *3* (40%)	102 + *3* (50%)	84 + *1–2* (75%)			
Asn	133 + *6* (100%)	116 + *3* (25%)		87 + *4* (45%)	88 + *3* (15%)	74 + *3* (80%)		
Gln	147 + *6* (90%)	130 + *3* (100%)		101 + *4* (15%)	84 + *1–2* (25%)			
Cys	122 + *5* (100%)	105 + *2* (35%)		76 + *3* (45%)	87 + *0* (15%)			
Met	150 + *4* (100%)	133 + *1* (30%)		104 + *2* (95%)	102 + *3* (30%)	61 + *0* (20%)	56 + *1–2* (45%)	
Phe	166 + *4* (100%)			120 + *2* (70%)				
Tyr	182 + *5* (100%)	165 + *2* (70%)		136 + *3* (85%)				
Trp	205 + *5* (100%)	188 + *2–4* (100%)						
His	156 + *5* (100%)			110 + *3–4* (100%)				
Lys	147 + *6* (100%)	130 + *3* (40%)			84 + *1* (100%)			
Arg	175 + *8* (100%)				116 + *3* (20%)	70 + *1* (45%)	60 + *6* (20%)	

versus 1.36 Å [26], respectively) and the activation energy (E_a) associated with the breaking of this bond is expected to be very low. It was calculated to be 3 kJ/mol by Uggerud [26]. These calculations locate the transition state associated with proton transfer 3 kJ/mol higher in energy than the OH-protonated form.

The third step of the fragmentation is the loss of CO from a $H_2NCH_2C^+=O$ ion not experimentally observed. The direct elimination of two neutral species (here H_2O and CO) without detecting any intermediate ion means that the latter is produced near or above its dissociation limit, or that is not a stable species. The enthalpy of reaction (1) was

Table 2
Ab initio calculated relative energies of $GlyH^+$ isomers (in kJ/mol)

Level of theory	$AP(Gly_N)-AP(Gly_{CO})$	$AP(Gly_N)-AP(Gly_{OH})$	Ref.
MP2/6-31G*//HF/3-21G	75	180	[23]
MP2/6-31G*//HF/6-31G*	42	—	[24]
MP2/6-31G**	124	141	[26]
MP2/6-311+G(3df,2p)//MP2/6-311+G**	122	—	[25(a)]

$$H_2NCH_2C^+=O \rightarrow NH_2CH_2^+ + CO \qquad (1)$$

first estimated to be -6 kJ/mol by Tsang and Harrison [4]. It was later calculated (MP2/6-31G**//HF/6-31G*) to be -53 kJ/mol [27]. More recently, studies by van Dongen et al. [28] revealed that the $H_2NCH_2C^+=O$ ion should be considered as an electrostatically bound ion/molecule complex $[H_2NCH_2-CO]^+$. Finally, recent calculations by Uggerud [26] at the MP2/6-31G** level determined that the dissociation of $[H_2NCH_2-CO]^+$ into $[NH_2CH_2]^+$ and CO requires 19 kJ/mol. The overall energy required to form the immonium ion from $GlyH^+$ was calculated to be 163 kJ/mol, in reasonable agreement with the experimental threshold of 186 kJ/mol [16].

In addition to the loss of 46 u, the low energy CID spectrum of $GlyH^+$ shows a minor loss of CO (see Table 1). This fragmentation has been previously observed in the metastable ion spectrum of FAB-generated $GlyH^+$ [6,12]. This is consistent with the above picture since the initially formed ion–dipole complex $[NH_2CH_2C(O)-OH_2]^+$ may easily rearrange to a $[H_2O-NH_2CH_2CO]^+$ form [26]. The potential energy surface appears to be such that either loss of H_2O or CO or both may easily occur, depending on the experimental conditions.

In conclusion, protonation occurs on the most basic amino site of glycine. Fragmentation of $GlyH^+$ requires proton transfer to the hydroxyl group. This yields an ion–molecule intermediate which can either eliminate H_2O + CO or else CO + H_2O, depending upon the lifetime of the intermediate, which is determined by the specific experimental conditions. In any case, fragmentation of the OH-protonated isomer is a very low energy process.

3.2. Other amino acids

Among the other protonated amino acids, the formation of the immonium ion is (see Table 1): (1) the unique or vastly dominant decomposition pathway for all aliphatic amino acids (Ala, Val, Leu, Ile, and Pro), Phe, and His; (2) not observed from $TrpH^+$, $LysH^+$, and $ArgH^+$; and (3) in competition with losses of other small molecules for all other α-amino acids. After total H/D exchange, all AAD^+ giving the immonium ion lose D_2O and CO exclusively, except for $HisD^+$. This is in good agreement with the above mechanism for the fragmentation of $GlyH^+$, because only exchangeable hydrogens are involved in the elimination of H_2O + CO. Therefore, we postulate that the formation of the immonium ion involves a common mechanism for all AAH^+ except for $HisH^+$: initial protonation at the N terminus followed by proton transfer to the hydroxyl group leading to fragmentation. This is consistent with the fact that for all AAs except for Trp, His, Lys, and Arg, the most basic site is expected to be the N terminus, i.e. the side chain functional groups are less basic than a primary amine.

The proton affinities of Trp, His, Lys, and Arg are the largest of all AAs: 949, 988, 996, and 1051 kJ/mol, respectively [29], which better corresponds to a side chain protonation. This will probably make proton transfer to the hydroxyl group a fairly unfavorable process. Therefore, immonium formation may disappear, provided that other mechanisms with smaller activation barriers are available. Our contention is that this is the case for Trp, Lys, and Arg, but not for His.

As discussed above, the glycine mechanism cannot apply directly to the loss of H_2O + CO from $HisH^+$.
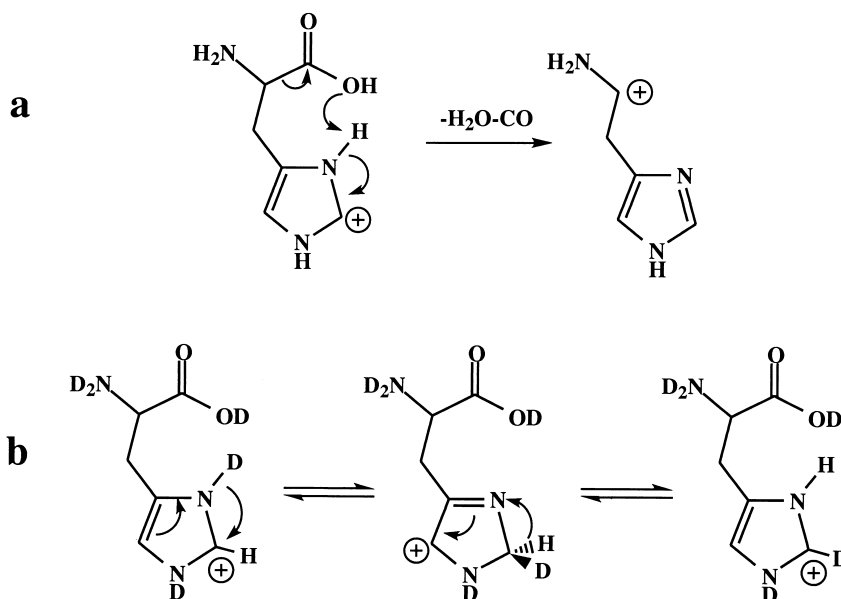
Scheme 1. Competitive losses of small molecules.

Furthermore, after H/D exchange of the labile hydrogens, $HisD^+$ loses competitively $D_2O + CO$ and $HDO + CO$ in a 3:1 ratio, pointing to a partial scrambling occurring before the elimination of water. The mechanism we propose involves proton transfer from the imidazole ring to the hydroxylic oxygen to yield OH-protonated Histidine, which then eliminates H_2O and CO as in the glycine mechanism [Scheme 1(a)]. In the heterocyclic ring, a scrambling between the two exchangeable hydrogens and the one located between the two nitrogen atoms explains the competitive losses of $D_2O + CO$ and $HDO + CO$ [Scheme 1(b)].

For several amino acids bearing a functional group on the side chain, the formation of the immonium ion is in competition with the loss of other small molecules: ammonia from $CysH^+$, $MetH^+$, $AsnH^+$, $GlnH^+$, and $TyrH^+$, or water from $SerH^+$, $ThrH^+$, $AspH^+$, and $GluH^+$. After H/D exchange of all labile hydrogens in the AAH^+ ions, the molecules of ammonia or water eliminated include exclusively deuteria atoms. The situation is different for $PheH^+$ on the one hand (exclusive loss of $H_2O + CO$), and for $TrpH^+$, $LysH^+$, and $ArgH^+$ on the other (loss of $H_2O + CO$ not observed).

Fragmentation mechanisms will first be investigated in detail for $SerH^+$ and $CysH^+$ and then extended to other AAH^+.

3.2.1. SerH⁺ and CysH⁺

The observed fragment ions formed by collisional activation of $SerH^+$ and $CysH^+$ are shown in Figs. 1 and 2, respectively, as a function of collision energy in the laboratory frame. In both cases, loss of $H_2O + CO$ is important, and even dominant for $SerH^+$. This is accompanied by an intense loss of NH_3 in the case of $CysH^+$; the apparent threshold for this loss is close to that for loss of $H_2O + CO$. With increasing collision energy, there appears to be a secondary fragmentation, whereby loss of H_2O follows NH_3 elimination. These are the main low energy fragmentation products of $CysH^+$. It should be noted that there is no sign of an elimination involving the side chain, such as loss of H_2S. The picture is different for $SerH^+$, for which loss of $H_2O + CO$ is largely dominant. The competitive fragmentation in this case is loss of H_2O, while loss of NH_3 is not observed. Loss of H_2O involving the alcohol group on the side chain is expected to occur since it has been established for the similar case of $ThrH^+$ via ^{18}O labelling experiments
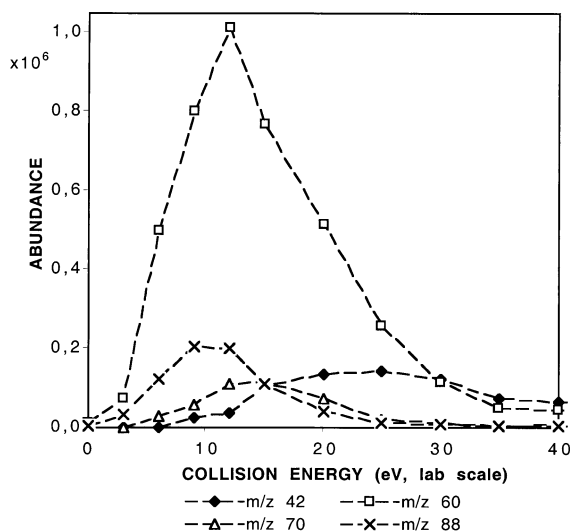
Fig. 1. Breakdown graph for the fragmentations of protonated serine.

[30]. However, involvement of the carboxyl group cannot be excluded. Detailed quantum chemical calculations were carried out to elucidate the structural and energetic characteristics of these fragmentations, and to explain the contrasted behaviors of $SerH^+$ and $CysH^+$.
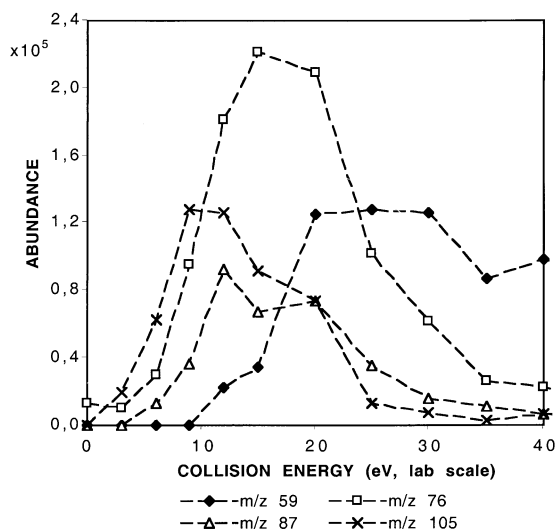

Fig. 2. Breakdown graph for the fragmentations of protonated cysteine.

Scheme 2 summarizes the three possible fragmentation pathways for $SerH^+$ and $CysH^+$. Starting from the most stable N-protonated isomer M_1, path **a** involves proton transfer to the carboxyl OH to yield isomer M_2. By analogy with $GlyH^+$, M_2 is expected to fragment very easily via elimination of H_2O + CO, with various possible structures A_n for the associated ion. Path **b** corresponds to direct loss of NH_3 from the initial M_1, giving ions denoted B_n. Finally, path **c** involves proton transfer to the side chain alcohol or thiol to form isomer M_3. Loss of HX (X = OH for $SerH^+$ and SH for $CysH^+$) may then occur, associated with the formation of ions C_n.

In order to clarify the mechanisms for these three channels, we have computed the relative energies of the various AAH^+ isomer ions M_n, several structures for each of the A_n, B_n, and C_n product ions, and the most important transition states along the various pathways. They are gathered in Tables 3 and 4 for $SerH^+$ and $CysH^+$, respectively. The optimized structures for M_1, M_2, and M_3 are shown in Fig. 3 for $SerH^+$ and in Fig. 4 for $CysH^+$.

3.2.1.1. Path **a**. As previously demonstrated for $GlyH^+$, the OH-protonated isomer M_2 is a loosely bound ion-neutral complex between an acylium ion and H_2O, with a C–O distance of 2.4 Å. On the contrary, side chain protonation in M_3 leads to a much more limited C–O bond elongation in serine (1.52 Å in M_3 versus 1.42 Å in M_1) and essentially no change in cysteine. This is understandable since the corresponding carbocations are not stabilized. The energy difference between M_1 and M_2 is computed to be 156 kJ/mol for $SerH^+$ and 163 kJ/mol for $CysH^+$. A value of 135 kJ/mol was obtained for $CysH^+$ by O'Hair et al. at a slightly lower level [31(b)]. These values are fairly similar to those for $GlyH^+$: 174 kJ/mol at the same level as in the present work [32], and 141 kJ/mol by Uggerud [26]. Therefore the energy difference between M_1 and M_2 can be considered to be roughly the same for a number of AAH^+. Furthermore, it appears that the transition state for this proton transfer lies close in energy to the OH-protonated minimum M_2: differences of 6 and 10 kJ/mol were computed for

Scheme 2.

GlyH$^+$ by Uggerud [26] and for CysH$^+$ by O'Hair et al. [31(b)], respectively.

For SerH$^+$ and CysH$^+$, the conceivable mechanisms are outlined in Scheme 3, together with the structures of the product ions A$_n$. Optimization of A$_1$-A$_4$ deriving from SerH$^+$ and CysH$^+$ leads to only two stable minima A$_1$ and A$_4$ (see Fig. 5). The most stable is the immonium ion A$_1$, which is stabilized by intramolecular interactions. The final energetics along this path for loss of H$_2$O + CO are somewhat dependent upon the amino acid considered. Loss of H$_2$O + CO from M$_2$ was computed to cost 22 kJ/mol for GlyH$^+$ [26]. In this work it has been estimated to be -10 and -18 kJ/mol for SerH$^+$ and CysH$^+$, respectively. Because of this extra stabilization of the immonium ion relative to the glycine case, the M$_2$

intermediate is now less stable than the dissociation products. This is in agreement with previous results by O'Hair et al. [31(b)]. Therefore the energy of M$_2$ will be taken as an approximation to the energy requirement for loss of H$_2$O + CO from other AAH$^+$ (vide infra).

3.2.1.2. Path **b**. The structures of the product ions B$_n$ and some of the associated transition states are shown in Fig. 6 for SerH$^+$ and Fig. 7 for CysH$^+$. As shown in Scheme 4, the M$_1$ isomer may eliminate ammonia via several mechanisms. Simple C–N bond breaking (leading to B$_1$ ions) is worth 360 and 333 kJ/mol for SerH$^+$ and CysH$^+$, respectively. Such a process is expected to be highly energetic because it leads to an unstable carbocation with a neighboring carboxyl

Table 3

Absolute energies (in hartrees) and relative energies (in kJ/mol) of the isomers of protonated serine and of the various final states associated with the losses of $H_2O + CO$, NH_3, and H_2O. The most stable N-protonated isomer M_1 is taken as the reference

Ions of serine	E (MP2(FC)/6-31G*)	ΔE MP2(FC)/6-31G* //MP2(FC)/6-31G*	ΔE MP2(FC)/6-31G* //MP2(FC)/6-31G* + ZPVE	Empirical $\Delta\Delta H^a$
M_1	−398.148197	0	0	0^b
M_2	−398.080576	177	156	161^c
M_3	−398.093192	144	136	111^d
$A_1 + H_2O + CO$	−398.078184	184	146	107^e
$A_2 + H_2O + CO$	collapses to A_1	—	—	
$A_3 + H_2O + CO$	collapses to $H_3N^+CH_2CH=O$	—	—	
$A_4 + H_2O + CO$	−398.056952	240	205	
$B_1 + NH_3$	−398.000748	397	+ 360	216^f
$B_2 + NH_3$	−398.065943	216	+ 192	107^g
$B_3 + NH_3$	−398.038044	289	+ 268	197^h
TS ($M_1 \rightarrow B_2 + NH_3$)	−398.045810	269	+ 245	
$C_1 + H_2O$	collapses either to C_2 or C_3	—	—	$239\ (252)^i$
$C_2 + H_2O$	−398.110637	99	75	-8^j
$C_3 + H_2O$	−398.117726	80	55	-14^k
$C_4 + H_2O$	−398.08815	158	138	97^l
TS ($M_3 \rightarrow C_2 + H_2O$)	−398.049446	259	238	
TS ($M_3 \rightarrow C_3 + H_2O$)	−398.046571	267	242	
TS ($M_3 \rightarrow C_4 + H_2O$)	−398.077984	184	171	

^{a} $\Delta\Delta H$ represents the difference in enthalpy between the final state and the N-protonated molecule. All energies are in kJ/mol. All ΔH_f^o used to estimate the ΔHs are from Ref. 21. The PA of neutral molecules are from Ref. 29.

^{b} The enthalpy of formation of $SerH^+$ protonated on the NH_2 group is calculated to be 54 kJ/mol from $\Delta H_f^o(Ser) = 561$ kJ/mol, PA(Ser) = 915 kJ/mol, and $\Delta H_f^o(H^+) = 1530$ kJ/mol.

^{c} $\Delta H_f^o(Ser(COOH)H^+) = \Delta H_f^o(NH_2CH(CH_2OH)C^+=O) - \Delta H_f^o(NH_2CH_2C^+=O) + \Delta H_f^o(Gly(COOH)H^+) = 215$ kJ/mol with $\Delta H_f^o(NH_2CH(CH_2OH)C^+=O) - \Delta H_f^o(NH_2CH_2C^+=O) \sim \Delta H_f^o(HOCH_2CH_2C^+=O) - \Delta H_f^o(CH_3C^+=O)$, and $\Delta H_f^o(HOCH_2CH_2C^+=O) = 441$ kJ/mol from $\Delta H_f^o(CH_3CH_2C^+=O) = 591$ kJ/mol corrected with the Benson increments for a OH replacing a methyl hydrogen. $\Delta H_f^o(CH_3C^+=O) = 653$ kJ/mol; $\Delta H_f^o(Gly(COOH)H^+) = \Delta H_f^o(GlyNH^+) + 174\ (32) = 427$ kJ/mol.

^{d} Difference in PA between Gly and ethanol (887 kJ/mol − 776 kJ/mol).

^{e} $\Delta H_f^o(NH_2CH^+CH_2OH) = 514$ kJ/mol from $\Delta H_f^o(NH_2CH^+CH_3) = 657$ kJ/mol corrected with the Benson increments for CH_2OH replacing CH_3.

^{f} $\Delta H_f^o(HOCH_2CH^+COOH) = 316$ kJ/mol from $\Delta H_f^o(CH_3CH^+COOCH_3) = 480$ kJ/mol corrected with the Benson increments for OH replacing the OCH_3 and for CH_2OH replacing CH_3.

^{g} $\Delta H_f^o(HOCH^+CH_2COOH) = 207$ kJ/mol from $\Delta H_f^o(HOCH^+CH_2CH_3) = 550$ kJ/mol corrected with the Benson increments for COOH replacing CH_3.

^{h} $\Delta H_f^o(cyclic{-}^+OHCH_2CH(COOH){-}) = 297$ kJ/mol with $\Delta H_f^o(oxirane{-}2\ carboxylic\ acid) = -426$ kJ/mol from $\Delta H_f^o(oxirane{-}) = -53$ kJ/mol corrected with the Benson increments for a COOH group replacing one hydrogen and PA(oxirane) = 807 kJ/mol.

^{i} $\Delta H_f^o(NH_2CH(CH_2^+)COOH) = 535$ kJ/mol from $\Delta H_f^o((CH_3)_2CHCH_2^+) = 832$ kJ/mol corrected with the Benson increments for an NH_2 replacing one methyl and a COOH replacing the other methyl. In parentheses, difference in PA between Gly and ethanol (111 kJ/mol) added to the bond dissociation energy (BDE) of the $-CH_2{-}^+OH_2 = 141$ kJ/mol; BDE($-CH_2{-}^+OH_2$) = $\Delta H_f^o(CH_3CH_2^+) + \Delta H_f^o(OH_2) - \Delta H_f^o(CH_3CH_2^+OH_2) = 902{-}242{-}519$ (in kJ/mol) with $\Delta H_f^o(ethanol) = -235$ kJ/mol and PA(ethanol) = 776 kJ/mol.

^{j} $\Delta H_f^o(NH_2CH^+CH_2COOH) = 288$ kJ/mol calculated from $\Delta H_f^o(NH_2CH^+CH_2CH_3) = 636$ kJ/mol corrected with the Benson increments for COOH replacing CH_3.

^{k} $\Delta H_f^o(NH_2C^+(CH_3)COOH) = 282$ kJ/mol calculated from $\Delta H_f^o(NH_2C^+(OH)CH_3) = 429$ kJ/mol corrected with the Benson increments for COOH replacing OH.

^{l} $\Delta H_f^o(cyclic{-}NH_2CH_2CH^+(COOH)) = 393$ kJ/mol calculated with $\Delta H_f^o(aziridine{-}2{-}carboxylic\ acid) = -244.5$ kJ/mol from $\Delta H_f^o(aziridine) = 126.5$ kJ/mol corrected with the Benson increments for a COOH group replacing one hydrogen and PA(aziridine-2-carboxylic acid) = 893 kJ/mol from PA(aziridine) = 905.5 kJ/mol corrected with the PA difference between methylamine (899 kJ/mol) and glycine (886 kJ/mol). The enthalpies of formation of H_2O, CO, and NH_3 are −242, −111, and −46 kJ/mol, respectively.

Table 4

Absolute energies (in hartrees) and relative energies (in kJ/mol) of the isomers of protonated cysteine and of the various final states associated with the losses of $H_2O + CO$, NH_3, and H_2S. The most stable N-protonated isomer M_1 is taken as the reference

Ions of cysteine	E (MP2/6-31G*)	ΔE MP2(FC)/6-31G* //MP2(FC)/6-31G*	ΔE MP2(FC)/6-31G* //MP2(FC)/6-31G* + ZPVE	Empirical $\Delta\Delta H^a$
M_1	−720.750545	0	0	0^b
M_2	−720.679740	186	163	159^c
M_3	−720.701573	129	121	98^d
$A_1 + H_2O + CO$	−720.680797	183	145	98^e
$A_2 + H_2O + CO$	collapses to A_1	—	—	
$A_3 + H_2O + CO$	collapses to $H_3N^+CH_2CH=S$	—	—	
$A_4 + H_2O + CO$	−720.657436	244	210	
$B_1 + NH_3$	−720.613983	358	333	208^f
$B_2 + NH_3$	−720.676717	194	170	164^g
$B_3 + NH_3$	−720.674175	200	180	138^h
TS ($M_1 \rightarrow B_3 + NH_3$)	−720.692356	153	140	
$C_1 + H_2S$	collapses either to C_2 or C_3	—	—	271^i (294)
$C_2 + H_2S$	−720.702275	127	101	24^j
$C_3 + H_2S$	−720.709364	108	81	18^k
$C_4 + H_2S$	−720.679795	186	164	129^l
TS ($M_3 \rightarrow C_4 + H_2S$)	−720.667546	218	199	

^{a} $\Delta\Delta H$ is the enthalpy difference between the final state and the N-protonated molecule. All energies are in kJ/mol. All the ΔH_f^o used to estimate the $\Delta\Delta H$ are from Ref. 21. The PA of AA are from Ref. 29.

^{b} The enthalpy of formation of Cys protonated on the NH_2 group is calculated to be 244 kJ/mol from $\Delta H_f^o(Cys) = -383$ kJ/mol, PA(Cys) = 903 kJ/mol and $\Delta H_f^o(H^+) = 1530$ kJ/mol.

^{c} $\Delta H_f^o(Cys(COOH)H^+) = \Delta H_f^o(NH_2CH(CH_2SH)C^+=O) - \Delta H_f^o(NH_2CH_2C^+=O) + \Delta H_f^o(Gly(COOH)H^+) = 403$ kJ/mol with $\Delta H_f^o(NH_2CH(CH_2SH)C^+=O) - \Delta H_f^o(NH_2CH_2C^+=O) \sim \Delta H_f^o(HSCH_2CH_2C^+=O) - \Delta H_f^o(CH_3C^+=O)$ and $\Delta H_f^o(HSCH_2CH_2C^+=O) = 629$ kJ/mol from $\Delta H_f^o(CH_3CH_2C^+=O) = 591$ kJ/mol corrected with the Benson increments for SH replacing CH_3; $\Delta H_f^o(CH_3C^+=O) = 653$ kJ/mol; $\Delta H_f^o(Gly(COOH)H^+) = \Delta H_f^o(GlyNH^+) + 180$ (32) = 427 kJ/mol.

^{d} Difference in PA between Gly and ethanethiol (887 − 798 kJ/mol).

^{e} $\Delta H_f^o(NH_2CH^+CH_2SH) = 695$ kJ/mol from $\Delta H_f^o(NH_2CH^+CH_3) = 657$ kJ/mol corrected with the Benson increments for CH_2SH replacing CH_3.

^{f} $\Delta H_f^o(HSCH_2CH^+COOH) = 498$ kJ/mol from $\Delta H_f^o(CH_3CH^+COOCH_3) = 480$ kJ/mol corrected with the Benson increments for an OH group replacing OCH_3 and for CH_2SH replacing CH_3.

^{g} $\Delta H_f^o(HSCH^+CH_2COOH) = 454$ kJ/mol from $\Delta H_f^o(CH_3CH^+SH) = 823$ kJ/mol corrected with the Benson increments for CH_2COOH replacing CH_3.

^{h} $\Delta H_f^o(cyclic-HS^+CH_2CH–COOH) = 428$ kJ/mol) with $\Delta H_f^o(thiirane-2-carboxylic\ acid) = -282$ kJ/mol from $\Delta H_f^o(thiirane) = 82$ kJ/mol modified with the Benson increments for a COOH group replacing one hydrogen and PA(thiirane) = 807 kJ/mol.

^{i} $\Delta H_f^o(NH_2CH(CH_2^+)COOH) = 548$ kJ/mol from $\Delta H_f^o((CH_3)_2CHCH_2^+) = 832$ kJ/mol corrected with the Benson increments for an NH_2 replacing one methyl and a COOH replacing the other methyl. In parentheses this final state is calculated adding the difference in PA between the amine and the thiol groups (98 kJ/mol) to the bond dissociation energy (BDE) of the $–CH_2–^+SH_2 = 196$ kJ/mol calculated from the reaction BDE($–CH_2–^+SH_2$) = $\Delta H(CH_3CH_2^+SH_2) \rightarrow CH_3CH_2^+ + SH_2$.

^{j} $\Delta H_f^o(NH_2CH^+CH_2COOH) = 288$ kJ/mol calculated from $\Delta H_f^o(NH_2CH^+CH_2CH_3) = 636$ kJ/mol corrected with the Benson increments for a COOH group replacing CH_3.

^{k} $\Delta H_f^o(NH_2C^+(CH_3)COOH) = 282$ kJ/mol calculated from $\Delta H_f^o(NH_2C^+(OH)CH_3) = 429$ kJ/mol corrected with the Benson increments for COOH replacing OH.

^{l} $\Delta H_f^o(cyclic-NH_2CH_2CH^+(COOH)) = 393$ kJ/mol calculated with $\Delta H_f^o(aziridine-2-carboxylic\ acid) = -244.5$ kJ/mol from $\Delta H_f^o(aziridine) = 126.5$ kJ/mol corrected with the Benson increments for a COOH group replacing one hydrogen and PA(aziridine-2-carboxylic acid) = 893 kJ/mol from PA(aziridine) = 905.5 kJ/mol corrected with the PA difference between methylamine (899 kJ/mol and glycine 886 kJ/mol). The enthalpies of formation of H_2O, CO, NH_3, and SH_2 are −242, −111, −46 and −20 kJ/mol, respectively.
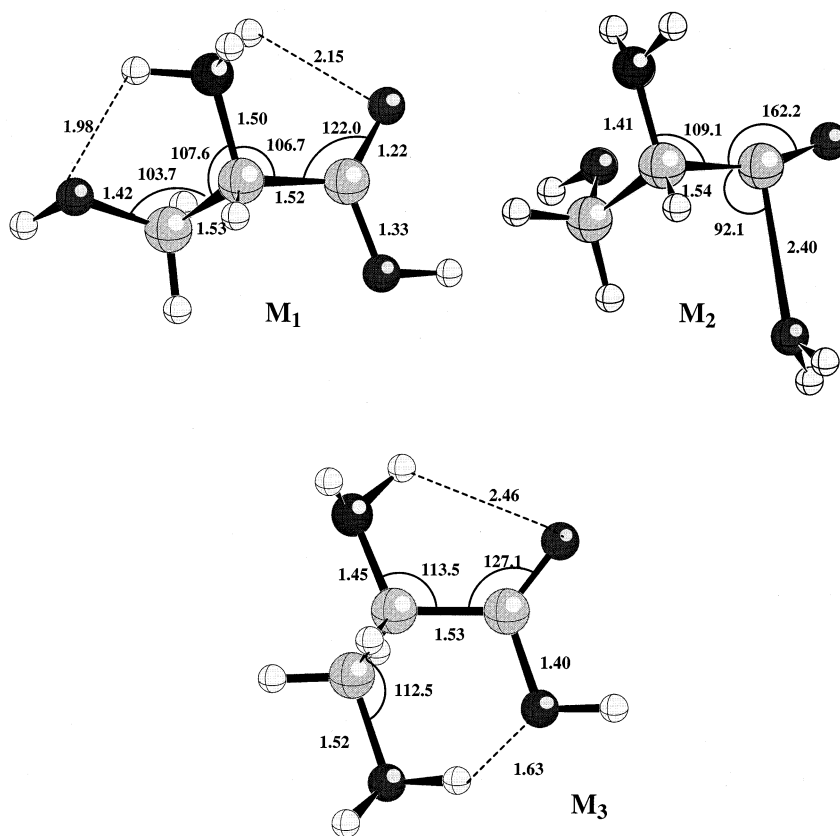
Fig. 3. Structures of SerH$^+$ isomers M$_n$.

group. Furthermore, the energetic similarity between SerH$^+$ and CysH$^+$ is also expected because the lateral chain is not involved in this mechanism. One way to stabilize the incoming carbocation is to assist NH$_3$ departure by a 1,2 H shift. The resulting carbocation B$_2$ is now stabilized by lone pair donation from X. This results in a much more favorable reaction enthalpy, again very similar for SerH$^+$ and CysH$^+$. A transition state for this process TS (M$_1$-B$_2$) (see Fig. 6) was optimized in the SerH$^+$ case. It involves a planar XCHCHCOOH skeleton with the migrating hydrogen out of plane, in an anti position relative to the leaving NH$_3$. The activation energy associated with this transition structure is high, 245 kJ/mol. Since the side chain is a spectator in this process, it is expected that the barrier is of comparable height for CysH$^+$. Therefore it was not computed. Finally, as

discussed by O'Hair et al. [31(b)], NH$_3$ elimination may be assisted by the X substituent, leading to the formation of a three-membered CXC ring (B$_3$ ions, see Figs. 6 and 7). The energy gaps between the B$_3$ and M$_1$ ions are 268 and 180 kJ/mol for SerH$^+$ and CysH$^+$. Therefore this path is of low energy for CysH$^+$ only. In the associated transition structure TS (M$_1$-B$_3$), a S–C bond is largely formed while the C–N bond is significantly stretched (see Fig. 7). This TS (140 kJ/mol higher in energy than M$_1$ for CysH$^+$) is connected to an ion-molecule complex with ammonia, which prefigures the final products. The final products lie higher in energy than the TS, making this path enthalpy-controlled. There are two possible dissociation pathways, as shown by O'Hair et al. [31(b)]. The enthalpically favored product ion is not B$_3$, but rather NH$_4^+$ formed by intracomplex proton transfer. Al-
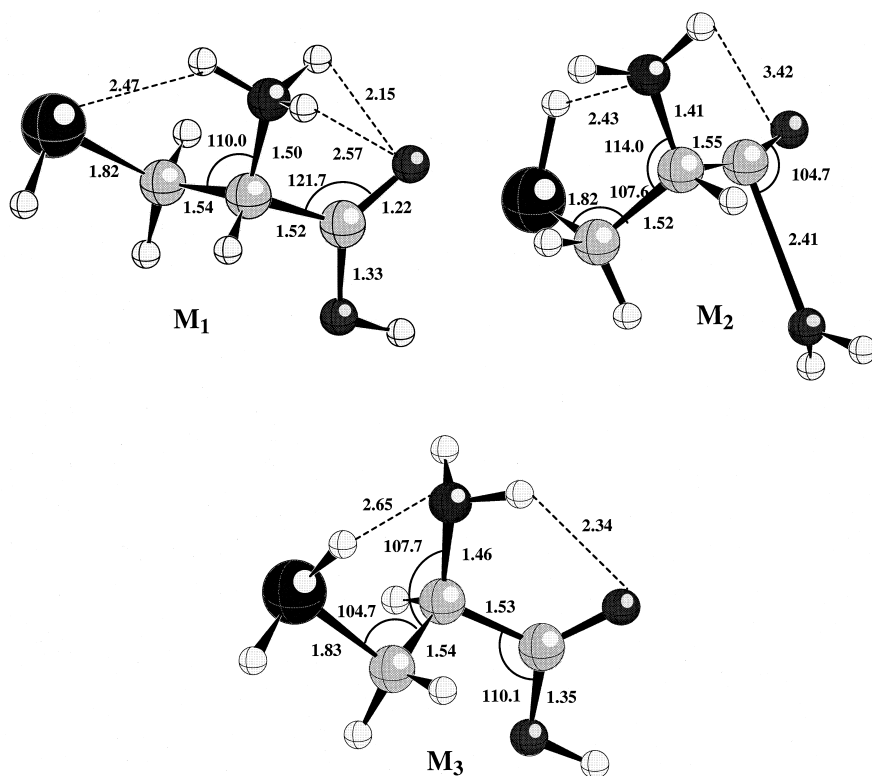
Fig. 4. Structures of CysH$^+$ isomers M$_n$.

though more favorable, this final state is a minor one in the results of O'Hair et al. This can be explained by the fact that in the transition state TS (M$_1$-B$_3$) leading to the ion-neutral complex, assistance of NH$_3$ departure by X requires an anti orientation of these groups, leading to an ion-neutral structure in which NH$_3$ is remote from the protonated sulfur. Therefore, proton transfer can occur only for species with long enough lifetimes. One then predicts that the relative amounts of NH$_4^+$ and B$_3$ ions formed will strongly depend upon experimental conditions.

The structures of ions B$_1$, B$_2$, B$_3$, and TS (M$_1$-B$_3$) may be compared to those obtained by O'Hair et al., which they named C, F, A and TSA, respectively. All are fairly similar within the differences expected for optimizations at the MP2 versus HF level. One difference is for B$_2$, where we have found a lower energy conformer involving a S-H–O hydrogen bond.

Here it is expected that the electronic differences

between oxygen and sulfur lead to significant differences in reaction energy profiles. The reaction enthalpies (which establish the energy requirement for this fragmentation pathway) are indeed quite different: 268 versus 180 kJ/mol for SerH$^+$ and CysH$^+$, respectively. This is not unexpected, given the larger size and better electron donation ability of sulfur relative to oxygen. It is this difference that forbids NH$_3$ elimination from SerH$^+$, while it is a major process for CysH$^+$.

3.2.1.3. Path **c**. The structures of the product ions C$_n$ are shown in Fig. 8 for SerH$^+$ and Fig. 9 for CysH$^+$. As shown in Scheme 5, the M$_3$ isomer may eliminate HX (X = OH, SH) via several mechanisms. Simple C–X bond breaking, which would lead to C$_1$ ions, does not lead to stable species. Geometry optimizations collapse instead to either C$_2$ or C$_3$ structures. The first involve 1,2 migration of the carboxyl group,

Scheme 3.
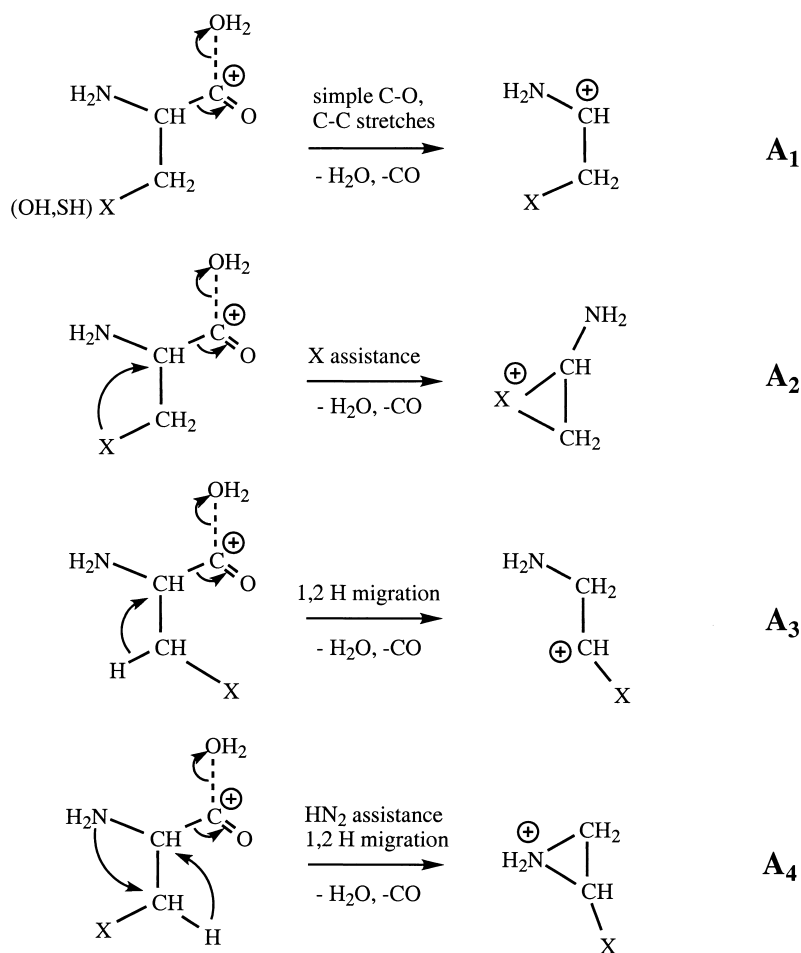
and the corresponding energies are 75 and 101 kJ/mol for SerH$^+$ and CysH$^+$, respectively. Another structural type found is C$_3$, which implies 1,2 hydrogen migration. Such fragmentations require 55 and 81 kJ/mol for SerH$^+$ and CysH$^+$, respectively. HX departure may also be assisted by three membered ring formation, yielding ions of type C$_4$, with associated energies of 138 and 164 kJ/mol, respectively. As for path **b**, formation of a three membered ring involving first row atoms is enthalpically unfavorable. Transition states for the formation of C$_2$-C$_4$ from M$_3$ were determined for SerH$^+$ (see Fig. 8). The energies of TS (M$_3$-C$_2$) and TS (M$_3$-C$_3$), which involve group transfer assisting H$_2$O elimination, are of high ener-

gies: 238 and 242 kJ/mol, respectively. Given the energetic similarities between SerH$^+$ and CysH$^+$ in such processes, analogous paths are also expected to be of high energy for CysH$^+$ and were not computed. The transition state TS (M$_3$-C$_4$) was also determined, and found to be the least demanding of the three, with an activation barrier of 171 kJ/mol. For CysH$^+$, the analogous transition state lies 199 kJ/mol above M$_1$ (see Fig. 9). Here again, the fact that it is the side chain that is eliminated makes the processes very similar for serine and cysteine. For both transition states and products, energies relative to M$_1$ are ~30 kJ/mol less stable for cysteine than they are for serine. This is due to the fact that in protonated ions involv-

a - SerH⁺-H₂O-CO
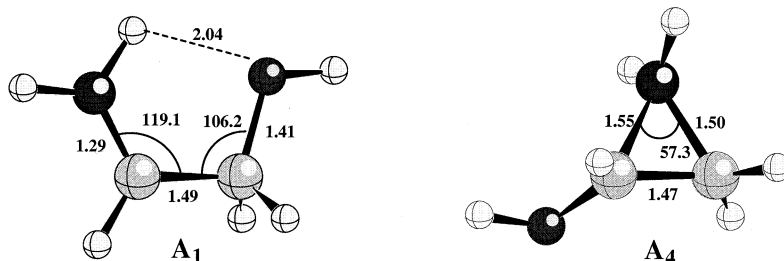
b - CysH⁺-H₂O-CO
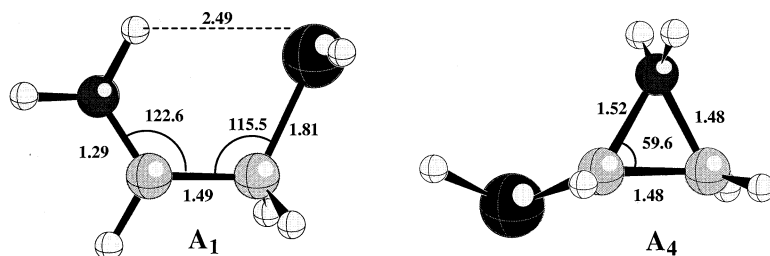
Fig. 5. A_n product ions in the fragmentations of SerH$^+$ and CysH$^+$.

ing a R$^+$-XH group, H$_2$O is a better leaving group than H$_2$S. In conclusion, the lowest energy pathway for HX elimination from SerH$^+$ and CysH$^+$ leads to a three membered ammonium ring, even though this is not a very stable product.

Based on the computations described above, we are now able to understand the contrasted unimolecular behaviors of SerH$^+$ and CysH$^+$. In the former case, the most favorable path for ammonia elimination passes through an activation barrier of 245 kJ/mol, while the lowest activation barrier for water elimination is worth 171 kJ/mol. With such a large difference, loss of NH$_3$ cannot compete with either H$_2$O loss from the side chain or H$_2$O + CO loss from the carboxyl group. The picture is reversed for CysH$^+$, with energy demands of 180 kJ/mol for NH$_3$ loss (final products) and 199 kJ/mol for H$_2$S loss (lowest transition state). In this case, participation of sulfur lone pairs stabilizes the former path to the

extent that H$_2$S loss cannot compete with either NH$_3$ or H$_2$O + CO eliminations.

The computed activation energies for the competitive processes are in qualitative agreement with the breakdown fragmentation graphs (see Figs. 1 and 2). Indeed, the apparent thresholds for loss of H$_2$O and of H$_2$O + CO from SerH$^+$ are similar (see Fig. 1), and their computed energetic requirements are 171 and 156 kJ/mol, respectively (the latter value is the relative energy of the isomer protonated on the C-terminal hydroxyl group). For CysH$^+$, the apparent thresholds for loss of NH$_3$ and of H$_2$O + CO are again similar, and the computed energy demands are 180 and 145 kJ/mol, respectively (here again, the latter value is the relative energy of the isomer protonated on the C-terminal hydroxyl group). At collision energies above threshold, the intensity of the [CysH-NH$_3$]$^+$ ion summed with that of its daughter [CysH-NH$_3$-H$_2$O]$^+$ ion is roughly the same as that of the [CysH-
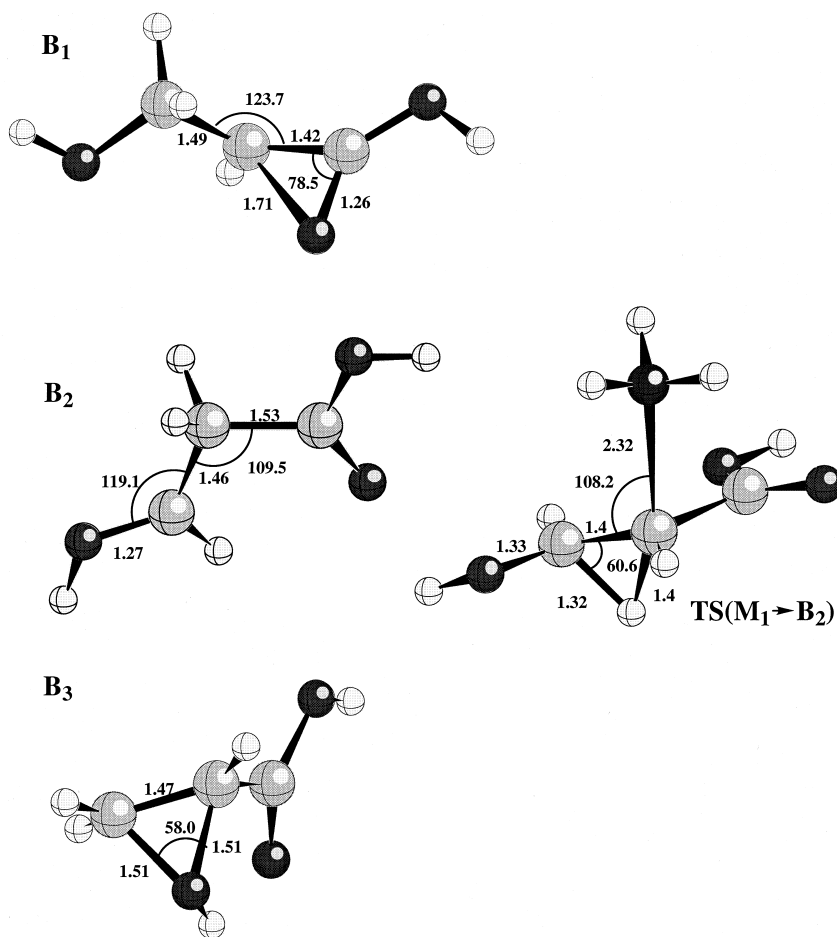
Fig. 6. B_n product ions and associated transition state in the fragmentations of SerH$^+$.

H_2O-CO]$^+$ immonium ion. This is at variance with the fragmentation of SerH$^+$, for which the immonium ion remains largely preponderant over a significant energy range. The low abundance of [SerH-H$_2$O]$^+$ (and fragment ions) may be explained by the reversibility of the proton transfer between NH$_2$ and the side chain OH, while that between NH$_2$ and the carboxyl OH may be considered to be irreversible because in this case proton transfer leads to an ion-molecule complex in which the CO$^+$–OH$_2$ bond is nearly broken.

3.2.1.4. Thermochemical estimates. The formation enthalpies of many ions are known [21]. When not available, an approximate value may be obtained by

combining the formation enthalpy of a structurally similar ion with increments for each additional functional group, as described by Benson [22]. This has been done for all minima involved in the possible fragmentations of SerH$^+$ and CysH$^+$. As shown by the results for SerH$^+$ and CysH$^+$ in Tables 3 and 4, respectively, this empirical approach cannot yield accurate enthalpies, yet it may provide relative energies that are good enough to understand the trends observed experimentally. The aim here is to evaluate the merits of this approximation procedure, in order to use it to understand the fragmentations of larger AAs for which a complete exploration of the potential energy surface would be a long and tedious task.

We have shown above that for some pathways, it is
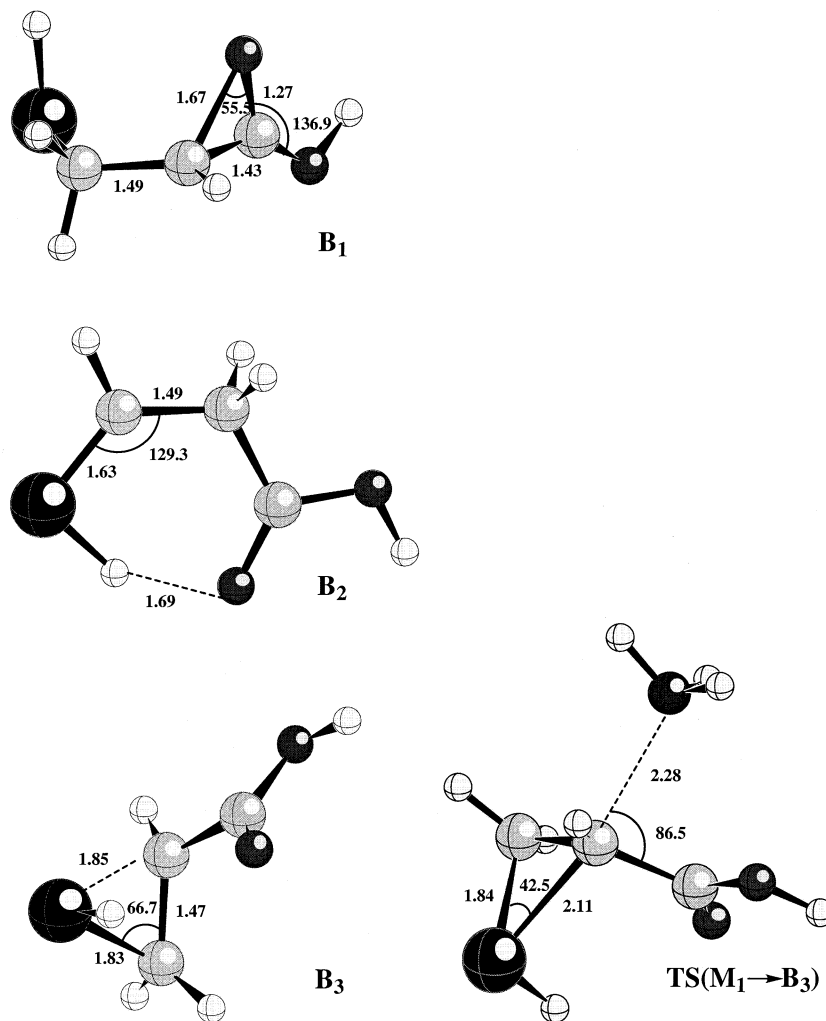
Fig. 7. B_n product ions and associated transition states in the fragmentations of $CysH^+$.

important to be able to evaluate transition state, not just minima. The empirical approach has been extended as follows: the detailed study of the fragmentations of $SerH^+$ and $CysH^+$ shows that all pathways involving rearrangements such as 1,2 hydrogen or group migration are unfavorable. All low energy paths involve a bond rupture at the protonated site. For the losses of NH_3 (from $CysH^+$) and H_2O (from $SerH^+$), elimination is assisted by a cyclization at the charged carbon atom of the incoming carbocation. We take advantage of this general behavior by making the rough estimate that the energy barrier lies halfway

between the structure resulting from simple bond breaking and that in which the carbocation is stabilized by cyclization. This procedure may be illustrated with an example. An upper value of the activation energy associated with the loss of H_2O from $SerH^+$ is given by the enthalpy difference between the N-protonated form M_1 and the hypothetical final state including the acyclic product ion C_1 (see Scheme 5) plus H_2O (239 kJ/mol). In order to include the stabilizing effect of NH_2 assistance via cyclization, we use the enthalpy average of C_1 and C_4 as an approximation to the true activation energy for this
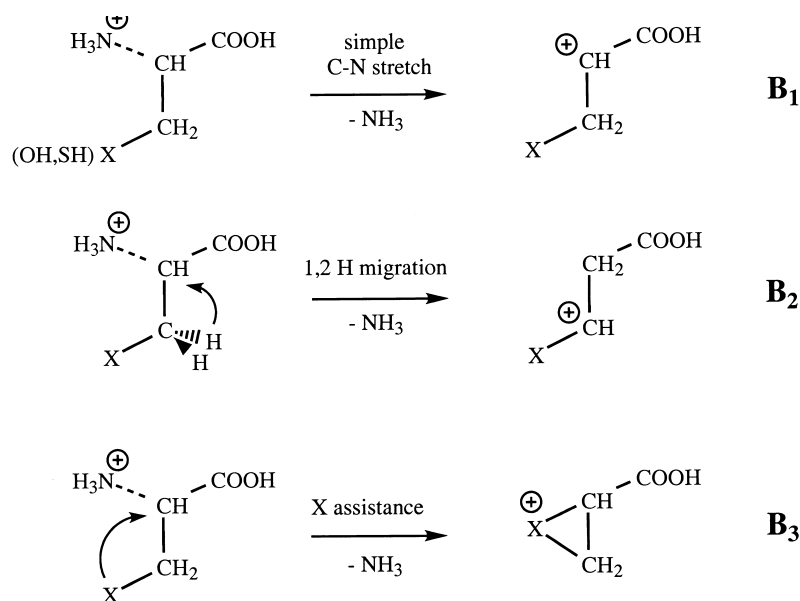
Scheme 4.

fragmentation, i.e. $(239 + 97)/2 = 168$ kJ/mol, to be compared to the MP2/6-31G* value of 171 kJ/mol. Although the very good agreement found in this case may be largely fortuitous, such estimates appear to be generally reasonable.

The same procedure has been applied to the losses of NH_3 and HX from $SerH^+$ and $CysH^+$. For $CysH^+$, the estimated energy demands are 173 and 200 kJ/mol, respectively, whereas they are 206 and 168 kJ/mol for $SerH^+$. For the loss of $H_2O + CO$, the estimated energy differences between M_1 and M_2 are 161 and 159 kJ/mol for $SerH^+$ and $CysH^+$, respectively. The conclusion is the same as that obtained above from the ab initio calculations: in agreement with the observed CID spectra (see Table 1), there are two "allowed" fragmentations for $SerH^+$, loss of H_2O from the side chain and loss of $H_2O + CO$ from the carboxyl group, while for $CysH^+$ the low energy processes are losses of NH_3 and of $H_2O + CO$.

3.2.2. $MetH^+$, $ThrH^+$, $AsnH^+$, $AspH^+$, $GlnH^+$, and $GluH^+$

$MetH^+$, $AsnH^+$, and $GlnH^+$ eliminate ammonia, as does $CysH^+$. For $MetH^+$ this necessarily involves

the N-protonated amine, whereas for $AsnH^+$ and $GlnH^+$, it may also occur from the amino group of the side chain. $ThrH^+$, $AspH^+$, and $GluH^+$ eliminate water as does $SerH^+$. For $ThrH^+$, exclusive loss of water from the side chain has been previously established by [18]O labelling experiments [30], and it is likely that the same holds for $SerH^+$. The resulting ion has been suggested to be a protonated aziridine [31(a)]. For $AspH^+$ and $GluH^+$, competition of side chain and carboxyl mechanisms is possible.

Mechanisms similar to those proposed for the primary fragmentations of $CysH^+$ and $SerH^+$ are expected to explain those of $MetH^+$, $ThrH^+$, $AsnH^+$, $AspH^+$, $GlnH^+$, and $GluH^+$ (Scheme 6). All start with the AAH^+ in its most stable form, in which the α-amino function is protonated. The first involves proton transfer to the carboxyl OH group, followed by consecutive losses of H_2O and CO, forming an immonium ion. Direct cleavage of the $C-NH_3^+$ bond may also occur, assisted by side chain cyclization. Finally, elimination of either H_2O, NH_3, or CH_3SH (depending upon the AA) may occur from the side chain, with the assistance of the amine function. As with $SerH^+$ and $CysH^+$, loss of $H_2O + CO$ is accom-
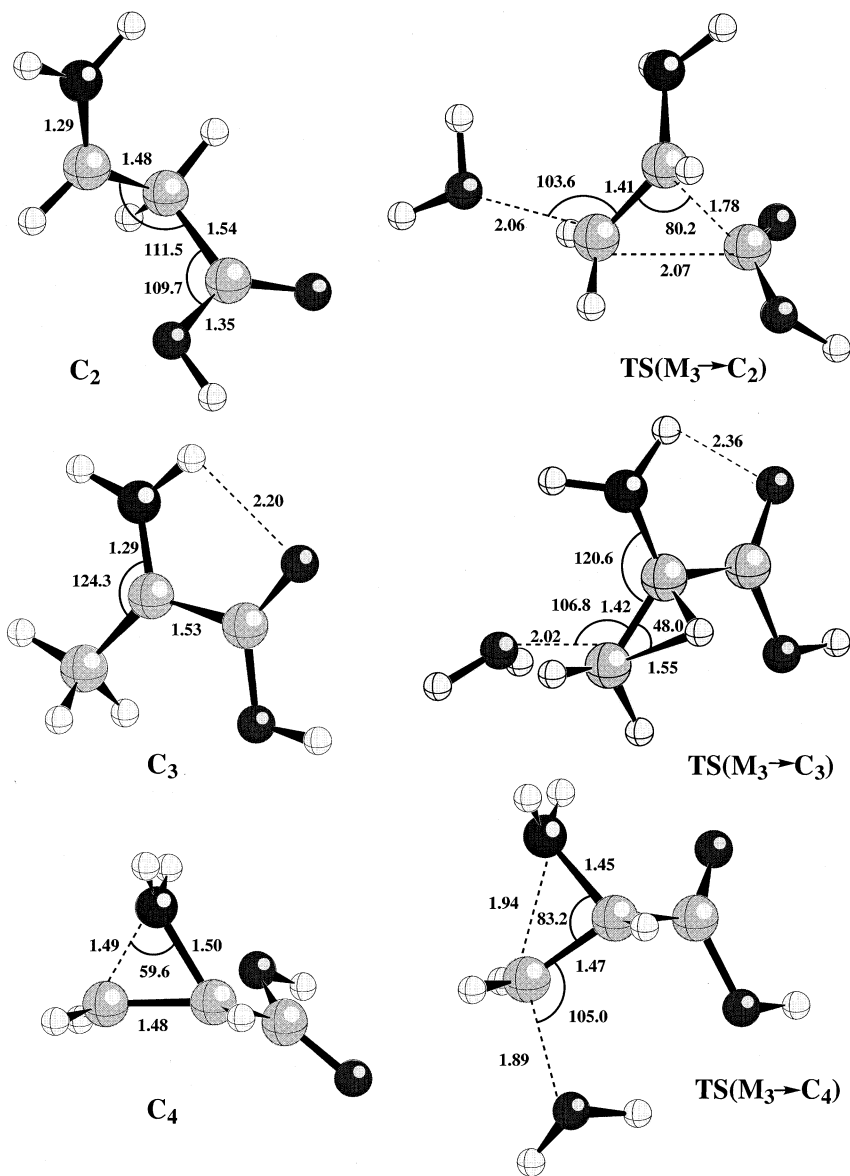
Fig. 8. C$_n$ product ions and associated transition states in the fragmentations of SerH$^+$.

panied by only one of the two other channels. In order to explain the outcome of this competition, the thermochemical approximation, which yielded results in good qualitative agreement with those of ab initio calculations for the decompositions of SerH$^+$ and CysH$^+$, was applied to mechanisms **b** and **c** for MetH$^+$, ThrH$^+$, AsnH$^+$, AspH$^+$, GlnH$^+$, and GluH$^+$. The estimated enthalpies of formation of the

linear and cyclic isomers of the product ions considered are detailed in Table 5. From these values, approximate activation energies for each fragmentation can be obtained as described above.

In the case of MetH$^+$, we did not find any ion with a structure close to that of the CH$_3$-cyclic-S$^+$(CH$_2$)$_2$CH-COOH ion and consequently its formation enthalpy has not been estimated. Compared to the

H_2N — COOH / CH / $\oplus$ CH_2 / HX $\xrightarrow[- HX]{\text{simple C-X stretch}}$ H_2N — COOH / CH / $\oplus$ CH_2 **C$_1$**

H_2N — COOH / CH / $\oplus$ CH_2 / HX $\xrightarrow[- HX]{\text{1,2 COOH migration}}$ H_2N $\oplus$ / CH / H_2C — COOH **C$_2$**

H_2N — COOH / H / $\oplus$ CH_2 / HX $\xrightarrow[- HX]{\text{1,2 H migration}}$ H_2N $\oplus$ — COOH / C / CH_3 **C$_3$**

H_2N — COOH / CH / $\oplus$ CH_2 / HX $\xrightarrow[- HX]{HN_2 \text{ assistance}}$ $\oplus$ H_2N — CH — COOH / CH_2 **C$_4$**

Scheme 5.
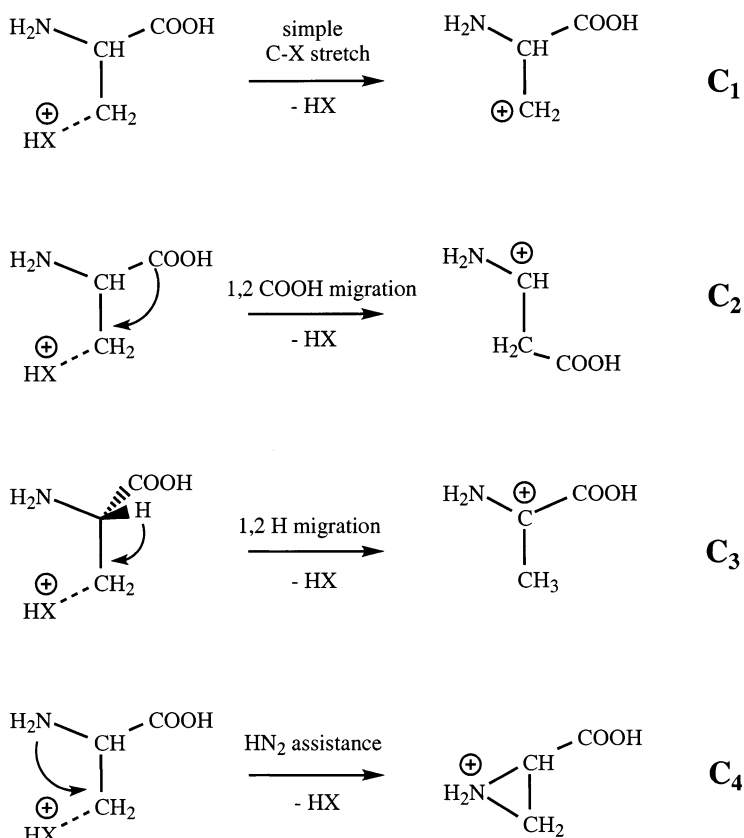
linear isomer, the stabilization due to cyclization is expected to be even larger than that for the analogous process in CysH$^+$. Therefore, loss of ammonia from the α-protonated amine is expected to be of much lower critical energy than loss of CH$_3$SH from the side chain. In agreement with this trend, loss of CH$_3$SH has a higher energy threshold than loss of NH$_3$ (from the breakdown fragmentation graph, not shown).

Estimated activation energies for NH$_3$ loss are 214, 206, 209, 164, and 172 kJ/mol for ThrH$^+$, AsnH$^+$, AspH$^+$, GlnH$^+$, and GluH$^+$, respectively. Those for HX loss from the side chain are 144, 186, 162, 144, and 115 kJ/mol, respectively. For these five AAH$^+$, the energy demand associated with the loss of HX from the side chain is always lower than that associated with the loss of NH$_3$ from the α-protonated amine. Therefore the loss of a small molecule from the side chain is predicted to be favored over NH$_3$ loss at the N terminus in all cases, except possibly for MetH$^+$. In agreement with these results, loss of ammonia is not observed in the CID spectra of ThrH$^+$, AspH$^+$, and GluH$^+$. For AsnH$^+$ and GlnH$^+$, loss of ammonia is predicted to be slightly more favorable via a side chain mechanism with a protonated amide intermediate, rather than via direct elimination from the protonated α-amino group. Although the product ion formed is the same in both mechanisms, our model implies that the α-amino mechanism is disfavored since it involves formation of a destabilized carbocation bearing an α-carboxy group.

Based on computations for SerH$^+$ and CysH$^+$ (vide supra), the activation energy for loss of H$_2$O + CO is estimated to be close to 160 kJ/mol. The
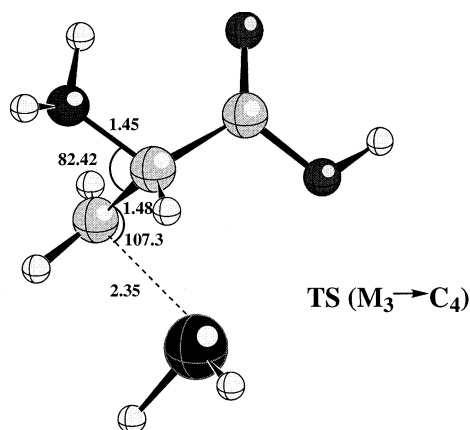
Fig. 9. Transition state associated with the formation of the C_4 product ion in the fragmentations of $CysH^+$. C_n product ions are identical with those of $SerH^+$ (see Fig. 8).

estimations discussed above show that this value lies close to or below (for $AspH^+$ and $AsnH^+$) or higher than (for $ThrH^+$, $GlnH^+$, and $GluH^+$) that for the side chain elimination process. On the other hand, it is lower than that for NH_3 loss from the N terminus, except for Gln. In agreement with the latter observation, loss of H_2O + CO is only a minor fragmentation in the CID spectra of $GlnH^+$ (see Table 1 and the breakdown graph [12]).

In summary, the main trends of the competition observed in the collisional activation processes of $CysH^+$, $SerH^+$, $MetH^+$, $ThrH^+$, $AsnH^+$, $AspH^+$, $GlnH^+$, and $GluH^+$ can be understood from the common picture described in Scheme 6. Simple thermochemical estimates of the activation barriers for each process are in good qualitative agreement with the observed fragmentations.

The secondary fragmentations of $SerH^+$, $CysH^+$, $ThrH^+$, and $MetH^+$ are deduced from the breakdown graphs presented in Figs. 1 and 2 and reference 12. $[CysH-H_3N]^+$ loses competitively H_2O and H_2O + CO, $[SerH-H_2O]^+$ decomposes to give $[SerH-2H_2O]^+$, and $[ThrH-H_2O]^+$ gives predominantly $[ThrH-2H_2O-CO]^+$. In the case of $MetH^+$, it is the immonium ion $NH_2CH^+(CH_2)_2SCH_3$ that generates competitively $CH_3SCH_2^+$ (*m/z* 61) by loss of $NH_2CH=CH_2$ and *m/z* 56 by loss of CH_3SH. The shifts of the latter to *m/z* 57 and *m/z* 58 in a 1:3 ratio

after total H/D exchange of labile hydrogens in the protonated molecule implies that the hydrogen transferred to the CH_3S group is either a labile hydrogen coming from NH_2 (1,5 H transfer) or a nonexchangeable hydrogen of the side chain (1,3 H transfer).

Breakdown graphs by Harrison and co-workers [12] showed the loss of ketene from $[AsnH-H_3N]^+$ and $[AspH-H_2O]^+$ giving *m/z* 74 and the loss of H_2O and CO from $[GlnH-H_3N]^+$ and $[GluH-H_2O]^+$ leading to *m/z* 84. However, in the CID spectra of $GlnH^+$ and $GluH^+$, after total H/D exchange of the labile hydrogens, the *m/z* 84 ion is shifted to *m/z* 85 and *m/z* 86 in a 2:3 ratio. The shift to *m/z* 85 is easily explained by a loss of D_2O + CO, which involves the OH group of the carboxyl function and a labile hydrogen from the α-amino group in agreement with a mechanism close to the one proposed earlier by Harrison. However, this mechanism does not explain the shift to *m/z* 86. The latter may be explained by a competitive loss of HDO involving a tautomeric form of the $[GluH-H_2O]^+$ and $[GlnH-NH_3]^+$ ions. The competitive losses of D_2O and CO and of HDO and CO are described in Scheme 7.

3.2.3. TyrH+ and PheH+

The proton affinities of $PheH^+$ and $TyrH^+$ is consistent with initial protonation occurring on the N terminus. Ammonia may then be lost directly, pro-
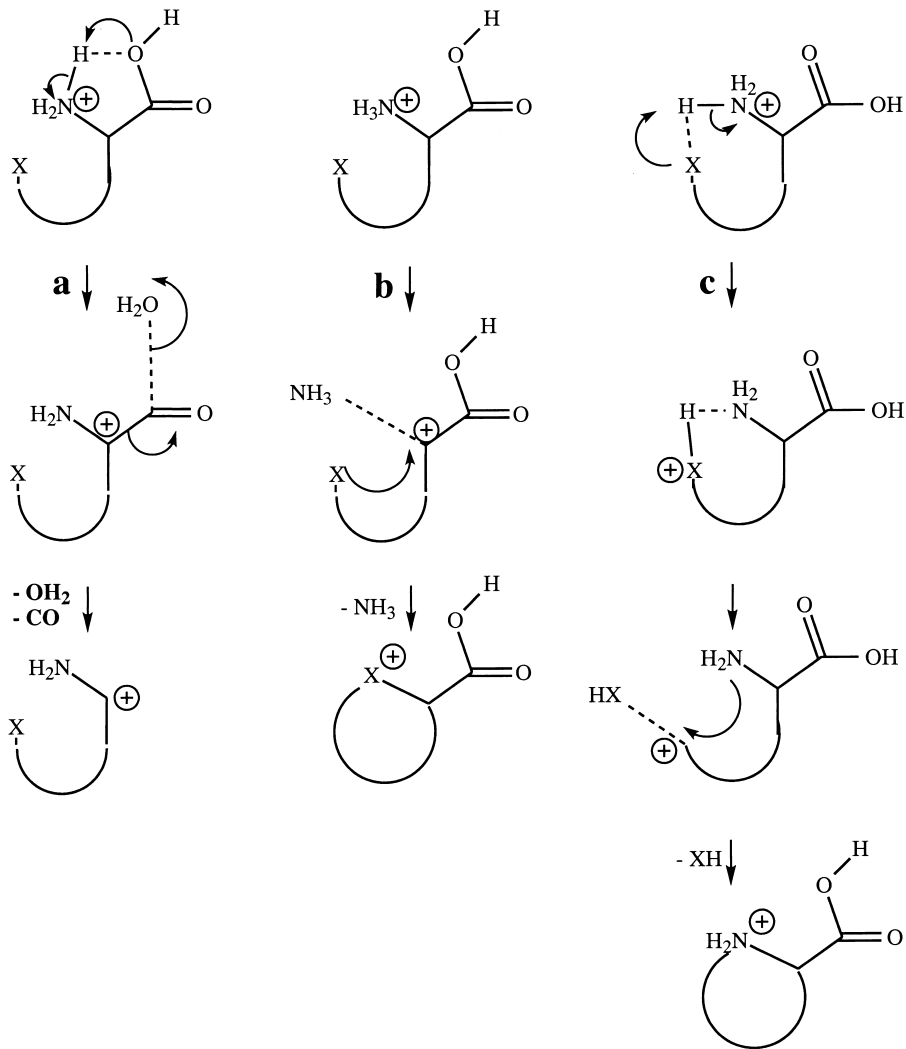
Scheme 6.

vided that the resulting carbocation is stabilized by the aromatic ring. Harrison et al. [12] have proposed such a mechanism, in which a phenonium ion is formed. This is consistent with the fact that NH_3 loss is observed to be intense for $TyrH^+$ but very weak for $PheH^+$. Their respective intensities are 80% and 5% relatively to the base peak AAH^+, at $E_{lab} = 9$ eV. Such phenonium ions are known to be strongly stabilized in quinoid forms by electron-rich substituents in the para position, as is the case for the phenol side chain of $TyrH^+$. In this case there is no proton
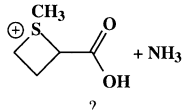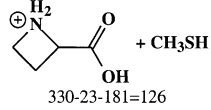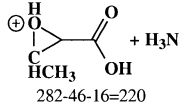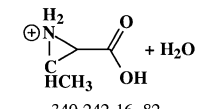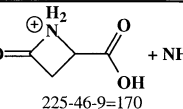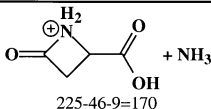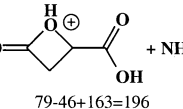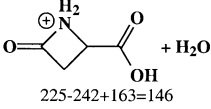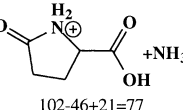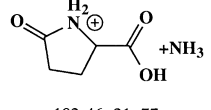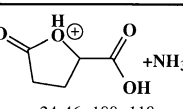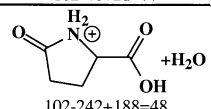
exchange between the amine and the ring, since exclusive loss of ND_3 is observed from $TyrD^+$ after H/D exchange of the labile hydrogens.

3.2.4. $TrpH^+$, $LysH^+$, and $ArgH^+$

$TrpH^+$ does not give the immonium ion after protonation. This result excludes an initial protonation on the α-amino group. In agreement with the high proton affinity of Trp (PA = 949 kJ/mol [29]), initial protonation is expected to occur on the side chain.

Table 5

Enthalpies of formation (experimental or estimated) of N-protonated Met, Thr, Asn, Asp, Gln, Glu (M_1), and energies of the following final states: $B_1 + NH_3$; $B_3 + NH_3$; $C_1 + XH$; $C_4 + XH$ relative to the corresponding M_1

M_1	$B_1 - NH_3$	$B_3 - NH_3$	$C_1 - XH$	$C_4 - XH$
$\Delta H_f^\circ(\text{MetH}^+)=181$	$CH_3S(CH_2)_2CH^+COOH$ $+ NH_3$ 464-46-181=237	+ NH_3 ? 282	$NH_2CH(COOH)CH_2CH_2^+{+}$ CH_3SH 547-23-181=343	+ CH_3SH 330-23-181=126
$\Delta H_f^\circ(\text{ThrH}^+)=16$	$HOCH(CH_3)CH^+COOH$ $+ NH_3$ 270-46-16=208	+ H_3N 282-46-16=220	$NH_2CH(COOH)CH^+CH_3$ $+ OH_2$ 465-242-16=207	+ H_2O 340-242-16=82
$\Delta H_f^\circ(\text{AsnH}^+)=9$	$H_2NCOCH_2CH^+COOH$ $+NH_3$ 273-46-9=242	+ NH_3 225-46-9=170	$NH_2CH(COOH)CH_2CO^+$ $+ NH_3$ 257-46-9=202	+ NH_3 225-46-9=170
$\Delta H_f^\circ(\text{AspH}^+)=-163$	$HOCOCH_2CH^+COOH$ $+NH_3$ 105-46+163=222	+ NH_3 79-46+163=196	$NH_2CH(COOH)CH_2CO^+$ $+ OH_2$ 257-242+163=178	+ H_2O 225-242+163=146
$\Delta H_f^\circ(\text{GlnH}^+)=-21$	$H_2NCO(CH_2)_2CH^+COOH$ $+NH_3$ 276-46+21=251	+NH_3 102-46+21=77	$NH_2CH(COOH)(CH_2)_2CO^+$ $+ NH_3$ 236-46+21=211	+NH_3 102-46+21=77
$\Delta H_f^\circ(\text{GluH}^+)=-188$	$HOCO(CH_2)_2CH^+COOH$ $+NH_3$ 84-46+188=226	+NH_3 - 24-46+188=118	$NH_2CH(COOH)(CH_2)_2CO^+$ $+ OH_2$ 236-242+188=182	+H_2O 102-242+188=48

All energetics in kJ/mol. Proton affinities are from Ref. 29. Enthalpies of formation of the molecules and of the reference ions are from Ref. 21. The influence of the COOH substituent on the proton affinities of cyclic product ions is taken into account by adding the PA difference between glycine and CH_3NH_2 (-13 kJ/mol).

Methionine: $\Delta H_f^\circ(\text{MetH}^+) = 181$ kJ/mol from $\Delta H_f^\circ(\text{Met}) = -414$ kJ/mol, PA(Met) = 935, and $\Delta H_f^\circ(\text{H}^+) = 1530$ kJ/mol. $\Delta H_f^\circ(CH_3S(CH_2)_2CH^+COOH) = 464$ kJ/mol is calculated from $\Delta H_f^\circ(CH_3CH^+COOCH_3) = 480$ kJ/mol corrected with the Benson increments for OH replacing OCH_3 and for $CH_3S(CH_2)_2$ replacing CH_3. $\Delta H_f^\circ(NH_2CH(COOH)CH_2CH_2^+) = 547$ kJ/mol is calculated from $\Delta H_f^\circ(CH_3CH_2CH_2^+) = 881$ kJ/mol corrected with the Benson increments for $(NH_2)CH(COOH)$ replacing CH_3. $\Delta H_f^\circ(\text{cyclic-}NH_2CH(COOH)CH_2CH_2^+{-}) = 320$ kJ/mol from $\Delta H_f^\circ(\text{cyclic-}NHCH(COOH)CH_2CH_2{-}) = -270$ kJ/mol calculated from $\Delta H_f^\circ(\text{azetidine}) = 99$ kJ/mol corrected with the Benson increments for COOH replacing one hydrogen of one carbon in α of the amine function and PA(cyclic-$NH_2CH(COOH)CH_2CH_2{-}) = 930$ kJ/mol (PA(azetidine) = 943 kJ/mol).

Threonine: $\Delta H_f^\circ(\text{ThrH}^+) = 16$ kJ/mol from $\Delta H_f^\circ(\text{Thr}) = -592$ kJ/mol and PA(Thr) = 922 kJ/mol. $\Delta H_f^\circ(HOCH(CH_3)CH^+COOH) = 270$ kJ/mol from $\Delta H_f^\circ(CH_3CH^+COOCH_3) = 480$ kJ/mol corrected with the Benson increments for OH replacing OCH_3 and $CH_3CH(OH)$ replacing CH_3. $\Delta H_f^\circ(\text{cyclic-}O^+(H)CH(CH_3)CH(COOH)) = 282$ kJ/mol from $\Delta H_f^\circ(\text{cyclic-}OCH(CH_3)CH(COOH)) = -458$ kJ/mol calculated from $\Delta H_f^\circ(\alpha\text{-methyl-oxirane}) = -95$ kJ/mol corrected with the Benson increments for COOH replacing one hydrogen of the methylene group and PA(cyclic-$OCH(CH_3)CH(COOH)) = 790$ kJ/mol (PA(α-methyl-oxirane) = 803 kJ/mol). $\Delta H_f^\circ(NH_2CH(COOH)CH^+CH_3) = 465$ kJ/mol is calculated from $\Delta H_f^\circ(CH_3CH^+CH_3) = 799$ kJ/mol corrected with the Benson increments for COOH and NH_2 replacing two hydrogens of the methyl group. $\Delta H_f^\circ(\text{cyclic-}^+NH_2CH(COOH)CH(CH_3){-}) = 340$ kJ/mol from $\Delta H_f^\circ(\text{cyclic-}NHCH(COOH)CH(CH_3){-}) = -278$ kJ/mol calculated from $\Delta H_f^\circ(\alpha\text{-methyl-aziridine}) = 91$ kJ/mol corrected with the Benson increments for COOH replacing one hydrogen of the methylene group and PA(cyclic-$NHCH(COOH)CH(CH_3){-}) = 912$ kJ/mol (PA(α-methyl-aziridine) = 925 kJ/mol).

Asparagine: $\Delta H_f^\circ(\text{AsnH}^+) = 9$ kJ/mol from $\Delta H_f^\circ(\text{Asn}) = -592$ kJ/mol estimated from $\Delta H_f^\circ(\text{Ala}) = -415$ kJ/mol corrected with the Benson increments for CH_2CONH_2 replacing CH_3 and PA(Asn) = 929 kJ/mol. $\Delta H_f^\circ(H_2NCOCH_2CH^+COOH) = 297$ kJ/mol is calculated from $\Delta H_f^\circ(CH_3CH^+COOCH_3) = 480$ kJ/mol corrected with the Benson increments for OH replacing OCH_3 and H_2NCOCH_2 replacing CH_3. $\Delta H_f^\circ(\text{cyclic-}^+NH_2COCH_2CH(COOH){-}) = 225$ kJ/mol from $\Delta H_f^\circ(\text{cyclic-}NHCOCH_2CH(COOH){-}) = -465$ kJ/mol calculated from $\Delta H_f^\circ(2\text{-azetidinone}) = -96$ kJ/mol corrected with the Benson increments for COOH replacing one hydrogen of one carbon in α of the nitrogen atom and PA(cyclic-$NHCOCH_2CH(COOH)) = 840$ kJ/mol (PA(2-azetidinone) = 853 kJ/mol). $\Delta H_f^\circ(H_2NCH(COOH)CH_2CO^+) = 257$ kJ/mol is calculated from $\Delta H_f^\circ(CH_3CH_2CO^+) = 591$ kJ/mol corrected with the Benson increments for COOH and NH_2 replacing two hydrogens of the methyl group.

(*continued*)
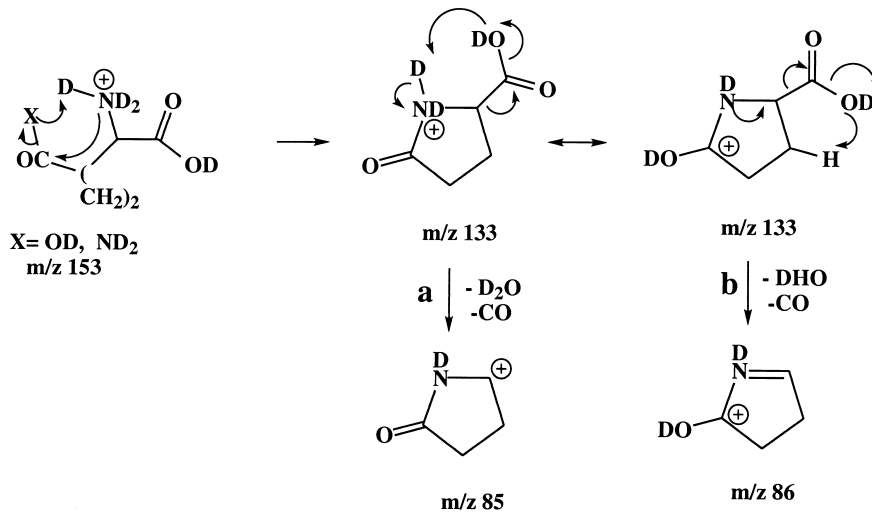
Scheme 7.

The protonating hydrogen may then be stabilized by the amino group.

The main fragmentation of TrpH$^+$ is a loss of ammonia to give the m/z 188 ion (see Fig. 10). This ion is shifted at m/z 190, 191, and 192 in a 2:4:1 ratio after total H/D exchange of the labile hydrogens. Harrison et al. [12] have proposed the assistance of the aromatic ring to help the elimination of NH$_3$ from

protonated aromatic AAs, via the formation of phenonium type ions. This interpretation is in agreement with the loss of ND$_3$ to give m/z 190 from TrpD$^+$ after total H/D exchange of the labile hydrogens. However, this mechanism does not explain: (1) the shifts to m/z 191 and 192; and (2) the lack of consecutive losses of H$_2$O and CO from TrpH$^+$. Given the high PA of Trp, we expect the protonation to occur on the nitrogen
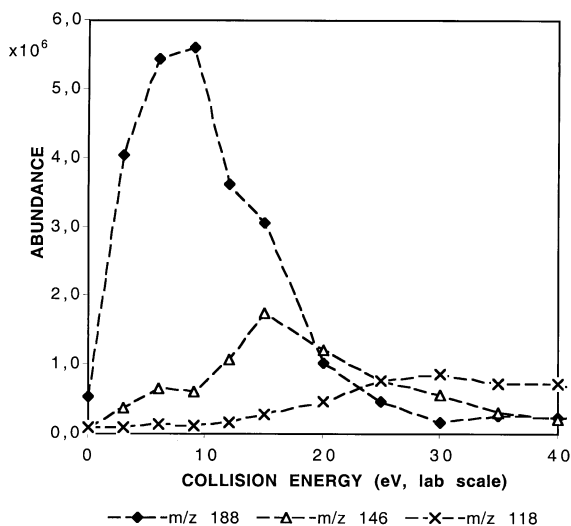
Fig. 10. Breakdown graph for the fragmentations of protonated tryptophan.

atom of the indole ring. Successive 1,2 proton transfers lead to a protonated form in which the proton is stabilized by the α-amino function (see Scheme 8). Reversible proton exchange between the aromatics and the amine leads to H/D scrambling, which explains the competitive losses of ND_3, ND_2H, and NDH_2 from H/D exchanged $TrpD^+$. Ammonia elimination may then be concerted with cyclization, forming a cation with a highly delocalized Π electron system. Although $HisH^+$ and $TrpH^+$ have strong similarities, the analogous elimination of NH_3 is disfavored with $HisH^+$ since the resulting carbocation cannot be stabilized. However, it is not clear why loss of $H_2O + CO$ is not observed at all with $TrpH^+$, since it is observed with $HisH^+$.

The main decomposition process of $LysH^+$ is the loss of ammonia. In $LysH^+$, the protonating hydrogen is probably bridged between the two NH_2 functions, explaining the great PA of Lys (957 kJ/mol [29]). The stabilization brought by this interaction is 71 kJ/mol comparing with the PA of glycine. As discussed above for other AAH^+, elimination of NH_3 is assisted by cyclization via the second amine. There are two possible processes: elimination of the protonated α-amino group with cyclization involving the side chain amine, or the other way around; both lead to the same cyclic final ion. [15]N labelling experiments [1,12] have shown that the ammonia lost specifically incorporates the nitrogen of the side chain. This can be understood with the model developed above for other AAH^+: ammonia elimination starts with C–N bond elongation, forming a transient cation, which will be stabilized by cyclization. The more stable the cation, the lower the activation energy. If the ammonia lost incorporated the α-amine, the transient carbocation would be destabilized by the COOH group, while this unfavorable effect is absent if the side chain nitrogen is eliminated.

Elimination of $H_2O + CO$ via proton transfer to the carboxyl OH group might not be more demanding than for other AAH^+ if proton transfer is assisted by the side chain amine. However, such a OH-protonated isomer would spontaneously transfer the proton to the side chain amine, leading back to the more stable N-protonated form. This is why loss of $H_2O + CO$ is not observed for $LysH^+$.

The cyclic $[LysH-NH_3]^+$ ion decomposes by loss of $H_2O + CO$ to give *m/z* 84, which is particularly intense in the CID spectrum shown in Table 1. The structure of $[LysH-NH_3]^+$, protonated pipecolic acid, is very similar to that of $ProH^+$. Therefore the same mechanism of $H_2O + CO$ loss applies as for all aliphatic amino acids. The same fragmentation has also been observed for protonated pipecolic acid by
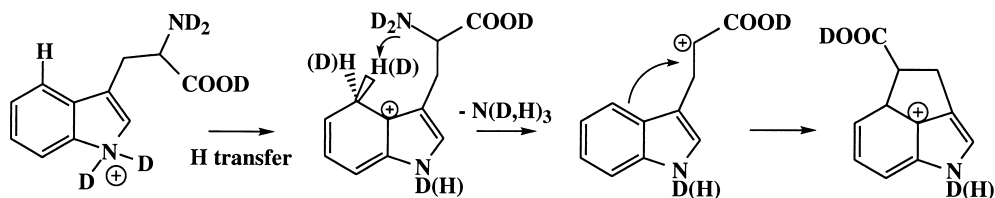
Scheme 8.
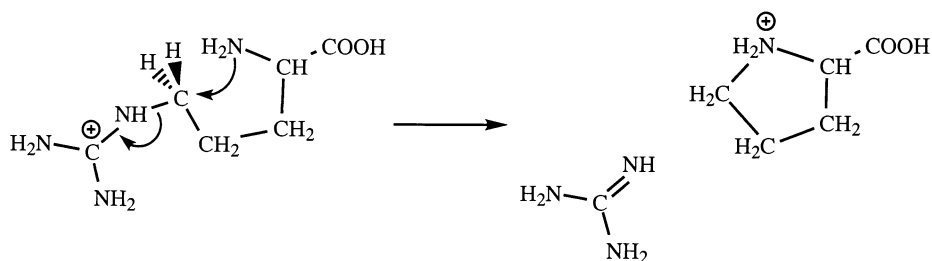
Scheme 9.

Yalcin and Harrison [33]. This brings additional support to the cyclic structure of [LysH-NH$_3$]$^+$.

The main reactions of ArgH$^+$ are the loss of a guanidine molecule to give the *m/z* 116 ion and the formation of protonated guanidine at *m/z* 60. An intense loss of H$_2$O + CO from the *m/z* 116 ion is also observed. A common intermediate may be invoked for the formation of these three fragments. Initial protonation is expected to occur at the imine nitrogen of guanidine, consistent with the high PA of Arg: 1051 kJ/mol [29]. The most favorable fragmentation involves heterolytic cleavage of the H$_2$C–NH bond, assisted by cyclization involving the α-amino group (Scheme 9). This leads to the formation of an ion–molecule complex between a substituted protonated pyrrolidine and neutral guanidine. Direct separation of these components leads to the *m/z* 116 ion. However, the PA of guanidine is 975 kJ/mol, while that of unsubstituted pyrrolidine is 948 kJ/mol [29]. On thermodynamic grounds, proton transfer to guanidine leading to the *m/z* 60 ion would be predicted, while the intensities of both ions are comparable (see Table 1). This can be understood by taking into account the fact that anchimeric assistance of guanidine elimination by the α-amino group is favorable in an anti orientation. As discussed previously for NH$_3$ loss from CysH$^+$, this leads to an unfavorable orientation of the ion-neutral complex, in which the molecule with high PA is remote from the proton (Scheme 9). The extent of proton transfer to guanidine will strongly depend upon the internal energy available and the flight time of the ions to the mass analyzer. This is apparent from the results of Harrison et al. [12]: metastable fragmentations lead to slightly

more intense *m/z* 60, while energy resolved CID spectra exhibit a dominant *m/z* 60 at low energies, but at higher energies *m/z* 116 becomes more intense.

4. Conclusion

The low energy CID spectra of all AAH$^+$ generated by electrospray ionization have been presented. There are very similar to the low energy CID spectra of FAB-generated AAH$^+$ of Harrison et al. [12]. A general picture for the major low energy fragmentations has been proposed. There are three possible decomposition pathways: (1) loss of H$_2$O + CO yielding an immonium ion, (2) loss of NH$_3$ from the N terminus, and (3) loss of a heteroatom-containing small molecule from the side chain. Out of the three, only one or two are observed for each AAH$^+$. The outcome of this competition has been explained by detailed ab initio calculations on SerH$^+$ and CysH$^+$, and thermochemical approximations for MetH$^+$, ThrH$^+$, GluH$^+$, GlnH$^+$, AspH$^+$, and AsnH$^+$. The model is consistent with the initial formation of the most stable isomer of AAH$^+$, protonated on the α-amino group for all AAH$^+$ except for TrpH$^+$, HisH$^+$, LysH$^+$, and ArgH$^+$. Proton transfer to one of the less basic groups prepares the elimination step, which is assisted by a neighboring basic group, leading to a cyclic product ion.

References

[1] G.W. Milne, T. Axenrod, H.M. Fales, J. Am. Chem. Soc. 92 (1970) 5170.
[2] P.A. Leclerq, D.M. Desiderio, Org. Mass Spectrom. 7 (1973) 515.

[3] M. Meot-Ner and F.H. Field, J. Am. Chem. Soc. 95 (1973) 7207.

[4] C.W. Tsang, A.G. Harrison, J. Am. Chem. Soc. 98 (1976) 1301.

[5] G. Bouchoux, S. Bourcier, Y. Hoppilliard, C. Mauriac, Org. Mass Spectrom. 28 (1993) 1064.

[6] S. Beranova, J. Cai, C. Wesdemiotis, J. Am. Chem. Soc. 117 (1995) 9492.

[7] A. Benninghoven, W.K. Sichtermann, Anal. Chem. 50 (1978) 1180.

[8] L. Liu, K.L. Busch, R.G. Cooks, Anal. Chem. 53 (1981) 109.

[9] T.D. Fan, E.D. Hardin, M.L. Vestal, Anal. Chem. 56 (1984) 1870.

[10] J.J. Zwinselman, N.M.M. Nibbering, J. Van der Greef, M.C. Ten Noever de Brauw, Org. Mass Spectrom. 18 (1983) 525.

[11] W. Kulik, W. Heerma, Biomed. Environ. Mass Spectrom. 15 (1988) 419.

[12] N.N. Dookeran, T. Yalcin, A.G. Harrison, J. Mass Spectrom. 31 (1996) 500.

[13] C.D. Parker, D.M. Hercules, Anal. Chem. 57 (1985) 698.

[14] C.D. Parker, D.M. Hercules, Anal. Chem. 58 (1986) 25.

[15] S. Bouchonnet, J.P. Denhez, Y. Hoppilliard, C. Mauriac, Anal. Chem. 64 (1992) 743.

[16] J.S. Klassen, P. Kebarle, J. Am. Chem. Soc. 119 (1997) 6552.

[17] (a) R. A. Dongre, J. L. Jones, A. Somogyi, V. H. Wysocki, J. Am. Chem. Soc. 118 (1996) 8365; (b) A.G. Harrison, T. Yalcin, Int. J. Mass Spectrom. Ion Processes 165/166 (1997) 339.

[18] Gaussian94 (Revision B.1), M.J. Frisch, G.W. Trucks, H.B. Schlegel, P.M.W. Gill, B.G. Johnson, M.A. Robb, J.R. Cheeseman, T.A. Keith, G.A. Petersson, J.A. Montgomery, K. Raghavachari, M.A. Al-Laham, V.G. Zakrzewski, J.V. Ortiz, J.B. Foresman, J. Cioslowski, B.B. Stefanov, A. Nanayakkara, M. Challacombe, C.Y. Peng, P.Y. Ayala, W. Chen, M.W. Wong, J.L. Andres, E.S. Replogle, R. Gomperts, R.L. Martin, D.J. Fox, J.S. Binkley, D.J. Defrees, J. Baker, J.J.P. Stewart, M. Head-Gordon, C. Gonzalez, J.A. Pople, Gaussian, Pittsburgh, PA, 1995.

[19] G. Schaftenaar, Univ. of Nijmemegen, URL:http://www.caos.kun.nl/~shaft/molden/molden.html.

[20] Copyright 1990, 1991, 1992, 1993, Research Equipment, Inc. d/b/a Minnesota Supercomputer Center, Inc. All rights reserved.

[21] S.G. Lias, J.E. Bartmess, J.F. Liebman, J.L. Holmes, R.D. Levin, W.G. Mallard, J. Phys. Chem. Ref. Data 17 (1988) (suppl. 1).

[22] S.W. Benson, Thermochemical Kinetics, Wiley, New York, 1976.

[23] S. Bouchonnet, Y. Hoppilliard, Org. Mass Spectrom. 27 (1992) 71.

[24] F. Jensen, J. Am. Chem. Soc. 114 (1992) 9533.

[25] (a) K. Zhang, A. Chung-Phillips, J. Chem. Inf. Comput. Sci. 39 (1999) 382; (b) K. Zhang, A. Chung-Phillips, J. Phys. Chem. A 102 (1998) 3625; (c) K. Zhang, A. Chung-Phillips, J. Comput. Chem. 19 (1998) 1862.

[26] E. Uggerud, Theor. Chim. Acta 97 (1997) 313.

[27] M.H. Lien, A.C. Hopkinson, J. Org. Chem. 53 (1988) 2150.

[28] W.D. van Dongen, W. Heerma, J. Haverkamp, C.G. de Koster, Rapid Comm. Mass Spectrom. 10 (1996) 1237.

[29] E.P.L. Hunter, S.G. Lias, J. Phys. Chem. Ref. Data 27 (1998) 413.

[30] W.D. van Dongen, C.G. de Koster, W. Heerma, J. Haverkamp, Rapid Comm. Mass Spectrom. 9 (1995) 845.

[31] (a) R.A.J. O'Hair, G.E. Reid, Rapid Comm. Mass Spectrom. 12 (1998) 999; (b) R.A.J. O'Hair, M.L. Styles, G.E. Reid, J. Am. Soc. Mass Spectrom. 9 (1998) 1275.

[32] F. Rogalewicz, Y. Hoppilliard, to be published.

[33] T. Yalcin, A.G. Harrison, J. Mass Spectrom. 31 (1996) 1237.